Using Disaster Induced Closures to Evaluate Discrete Choice Models of Hospital Demand*

Devesh Raval
Federal Trade Commission
draval@ftc.gov

Ted Rosenbaum
Federal Trade Commission
trosenbaum@ftc.gov

Nathan E. Wilson
Federal Trade Commission
nwilson@ftc.gov

November 16, 2020

Abstract

Diversion ratios play a large role in the assessment of mergers, but little is known about how well they are predicted by standard discrete choice models of demand. Using a series of natural disasters that unexpectedly removed hospitals from patients' choice sets, we evaluate this question for patients requiring inpatient care. We compare observed post-disaster diversion ratios to predicted diversion ratios estimated from pre-disaster data, and find that all of the standard demand models consistently underpredict large diversions. Both unobserved heterogeneity in preferences over travel and post-disaster changes to physician practice patterns can explain some of the underprediction of large diversions. We find a significant improvement using models with a random coefficient on distance.

JEL Codes: C18, I11, L1, L41

Keywords: hospitals, natural experiment, patient choice, diversion ratio, antitrust

*We would like to thank Jonathan Byars, Gregory Dowd, Aaron Keller, Laura Kmitch, and Peter Nguon for their excellent research assistance. We also wish to express our appreciation for audiences and our discussants – Nathan Miller, Yair Taylor, Alex Fakos, Rob Porter, Kate Ho, and Vincent Pohl – at the 2015 AEA Meetings, 2015 DC IO Day, 2015 IIOC, 2015 QME Conference, 2015 FTC Microeconomics Conference, and 2019 ASHEcon. This paper was previous circulated as "Industrial Reorganization: Learning About Patient Substitution Patterns from Natural Experiments". We would also like to thank Cory Capps, Chris Garmon, Marty Gaynor, Dan Hosken, Ginger Jin, Sam Kleiner, Francine Lafontaine, Jason O'Connor, Dave Schmidt, Charles Taragin, Bob Town, and anonymous FTC referees for their detailed comments on the paper, as well as editor Marc Rysman and two anonymous referees at RAND. The views expressed in this article are those of the authors. They do not necessarily represent those of the Federal Trade Commission or any of its Commissioners.

1 Introduction

Directly measuring the extent to which products are substitutes has become fundamental to horizontal merger analysis. One measure of substitutability is the diversion ratio, which, in the posted price context, is defined as the share of consumers who switch from one specific product to another in response to a marginal price change (Farrell and Shapiro, 2010). The US Department of Justice (DOJ) and Federal Trade Commission (FTC) added this metric to the 2010 Horizontal Merger Guidelines, characterizing it as a measure of "the extent of direct competition" between merging parties' products.

The FTC and DOJ now use diversion ratios outside of their original posted price context to characterize the intensity of competition between merging parties, adjusting the measure to reflect the price setting mechanism. In particular, the FTC regularly uses the choice-removal diversion ratio as a measure of substitutability in negotiated price settings like hospital markets (e.g., Farrell et al., 2011; Capps et al., 2019). Whereas the standard diversion ratio measures substitution in response to marginal price changes, the choice-removal diversion ratio is defined as the share of patients who switch from hospital A to hospital B if hospital A is no longer available in their choice set.

Ideally, one would estimate the choice-removal diversion ratio by observing the share of patients that would have chosen hospital A if it were available but instead go to hospital B after hospital A is removed from patients' choice sets. This is analogous to what would occur if the hospital were excluded from a private insurer's network of covered providers. However, exogenous breakdowns in contracting between hospitals and managed care organizations are

rarely, if ever, available. As a result, economists typically estimate choice-removal diversion ratios using discrete choice demand models that do not include this type of variation. Consequently, despite choice-removal diversion ratios' importance to the study of health care markets and antitrust policy, it is unknown how well frequently used econometric models recover them.

We address this question by comparing econometric models' predictions of choice-removal diversion ratios to observed diversion patterns following the unexpected closures of six different hospitals. Specifically, we exploit the effects of four natural disasters that temporarily closed a variety of hospital types (e.g., small community hospital, academic medical center, etc.) in urban, suburban, and rural markets. The natural disasters allow us to measure the recapture of the destroyed hospital's patients by other area hospitals. Our experimental setting thus approximates the counterfactual exercise of an insurer excluding a hospital from a network.

Using pre-disaster data, we estimate eight different demand models that have been used in research and policy analysis. All of these models are variations of the discrete choice logit framework. They differ in what assumptions are imposed about the role observable patient heterogeneity may play in determining hospital choices.

Across all of the disasters, we find that all of the demand models consistently underpredict choice-removal diversion to hospitals with large observed diversion ratios. A ten percentage point increase in the observed diversion ratio increases the gap between the predicted and observed diversion ratios by 3.5 to 4.3 percentage points. However, some models perform better at predicting choice-removal diversion ratios than others. Demand models that include as covariates alternative specific constants – a measure of vertical differentiation – and patient

travel time – a measure of horizontal differentiation – perform significantly better than those without either one of these elements. Among the models that include both of the elements, there is little difference in the accuracy of predictions of choice removal diversion ratios.

Differences in the disutility of travel across patients are one likely explanation for our findings. On average, we underpredict diversion to nearby hospitals, which could be due to patients of the destroyed hospital having a greater disutility of travel than the average patient in the service area. We account for such heterogeneity by estimating a random coefficient on travel time using the post-disaster variation, and find a 20 to 25% improvement in model performance. Given this improvement, one may want to include random coefficients in demand models even when rich microdata allows flexible controls for observed heterogeneity.

Another potential explanation for our findings is changes in the physicians that patients see. Typically, physician referrals are not included in models of hospital demand, including all of the models we estimate. We can, however, examine changes in physician labor supply using data on operating physicians for the New York disasters. For the NYU closure, we substantially underpredict diversion to the hospital that saw a large influx of NYU physicians post-disaster. In general, we find a massive decline in admissions associated with doctors from the destroyed hospitals. If patients went to different physicians after the disaster, demand post-disaster could be quite different than demand pre-disaster.

Overall, we add to the growing body of work using quasi-exogenous variation to assess the performance of econometric models. This literature stems from LaLonde (1986), and recent contributions include Todd and Wolpin (2006) and Pathak and Shi (2014). Within this literature, our article is most similar to that of Conlon and Mortimer (2018), who also use experimental data to evaluate diversion estimates. We view our respective analyses as

complementary. While both studies examine diversion ratios using variation arising from the elimination of a choice, Conlon and Mortimer (2018)'s setting is a posted price one, where the economically relevant diversion ratio is from a small price change. In contrast, we study a bargaining setting in which the diversion ratio of interest also involves removing a choice from consumers' choice sets. Moreover, we formally assess the role for unobservable heterogeneity even when rich data on consumer and product characteristics are available.

Our article also contributes to the literature on hospital competition and merger evaluation.[1] Our results suggest that using standard discrete choice demand models may be a useful, albeit imperfect, means of estimating choice-removal diversion ratios. As we have noted, these diversion ratios are an important input into hospital merger analysis. Providers and payers also use these models to predict demand for providers' services.

Finally, our article is related to Raval et al. (2019), which studies how machine learning models perform in changing choice environments. Using variation from the same set of natural disasters described in this article, that paper studies machine learning models' predictive accuracy for individuals' choices. In contrast, we focus here on traditional econometric models' performance in predicting aggregate diversion ratios and the policy implications of those estimates.

The article proceeds as follows. In Section 2, we briefly lay out why the choice-removal diversion ratio is a means of gauging the potential harm from horizontal mergers when prices are negotiated. We describe the disasters, research design, and data in Section 3, while we discuss the specifications we focus on in this article and model estimation in Section 4. In

[1] Studies include Capps et al. (2003), Gowrisankaran et al. (2015) and Garmon (2017), as well as the literature surveyed in Gaynor et al. (2015).

Section 5, we show that all of our models underpredict large diversions, but that some models do better than others. We examine explanations for why we underestimate large diversions in Section 6. Section 7 concludes.

2 Background

The marginal price change diversion ratio was derived in the context of posted-price markets in which consumers directly face price differences across products. However, in markets for health care providers, most patients do not directly face price differences across providers as long as providers are in patients' network of covered providers from their managed care organization (MCO). Given this dynamic, the antitrust analysis of these mergers has focused on provider competition for inclusion in MCO networks (Capps et al., 2019). We explain below why the choice-removal diversion ratio serves as an important quantitative metric for the post-merger loss of that competition.

The agencies, following the recent academic literature on hospital competition, model interactions between MCOs and health care providers as a series of independent bilateral negotiations over the price the MCO will pay for care provided to its beneficiaries that receive care at the provider.[2] In this framework, consider a market where two hospitals plan to merge. The pre-merger price paid to each hospital reflects the value each hospital contributed to the MCO's network. This value is a function of their substitutability to the other merging party as well as any additional hospitals in the network. If patients saw

[2] A "Nash-in-Nash" concept is typically used to model equilibrium outcomes. For the use of this approach by the US antitrust agencies, see Capps et al. (2019) or Farrell et al. (2011). For its use in the academic literature, see Gaynor et al. (2015), Gowrisankaran et al. (2015), or Ho and Lee (2017).

the two merging hospitals as particularly substitutable, the choice removal diversion ratios between them would be high. This would imply that the value each would add to an MCO's network in isolation is small. If one of the hospitals was excluded then those patients who would have gone to the newly excluded hospital would end up at the other with negligible loss in welfare.

Once the hospitals merge, however, the combined system will be in a much stronger position in its negotiations with the MCO. Now, rather than having the outside option be a network that still included many patients' (close substitute) second choice, the value of the MCO's outside option will depend upon the attractiveness of the remainder of its network to patients who lost their first two choices. The diminished value of this outside option leads to higher post-merger prices (Gaynor et al., 2015). If the system instead bargains on a hospital-by-hospital basis, its post-merger outside option if it fails to reach an agreement for one of the hospitals will internalize the recapture of many of the patients that would have gone to the excluded hospital. All else equal, this too will lead to higher post-merger negotiated prices (Garmon, 2017).

Thus, the choice-removal diversion ratio, our focus in this paper, captures the extent to which a given hospital is the second choice of another hospital's patients, which is the relevant notion of diversion for these markets. While the choice-removal diversion ratio is not discussed in the 2010 Horizontal Merger Guidelines, the close connection to how competition takes place in provider markets have led them to be used in the FTC's analysis of hospital mergers (Capps et al., 2019; Farrell et al., 2011), official FTC court filings in support of FTC challenges to hospital mergers, and in court by testifying experts.[3]

[3]For an expert report, see Capps et al. (2019, p. 453). For FTC complaints, see

3 Data

3.1 Disasters

To study the accuracy of estimated choice-removal diversion ratios, we use the unexpected closures of six hospitals following four natural disasters. Table Ia lists the locations of the disasters, when they took place, the nature of the event, and the hospital(s) affected. The Northridge earthquake destroyed St. John's Hospital in Santa Monica, a neighborhood of Los Angeles. Two tornadoes hit Sumter Regional Hospital in rural Georgia and Moore Medical Center in suburban Oklahoma City. Finally, Superstorm Sandy hit New York City and closed three hospitals – NYU Langone, Bellevue Hospital Center, and Coney Island Hospital. NYU Langone is one of the top academic medical centers in the country, Bellevue Hospital is the flagship of the New York City public hospital system, and Coney Island Hospital is the local hospital of the Coney Island neighborhood.

Our sample thus includes disasters affecting urban markets as well as rural markets, and elite academic medical centers as well as community health centers. A significant advantage of the heterogeneity in location and hospital type is that any results consistent across these different settings are likely to have high external validity.

Our analysis relies on comparing predictions based on models estimated on data from the period before the disaster ("pre-period") to admissions taking place after the disaster ("post-period"). Table Ib lists the closure and reopening dates for each of the destroyed

www.ftc.gov/enforcement/cases-proceedings/141-0191-d09368/penn-state-hershey-medical-center-ftc-commonwealth and www.ftc.gov/enforcement/cases-proceedings/1410231/ftc-v-advocate-health-care-network.

hospitals as well as our delineations of the pre- and post-periods for each of the hospitals. We exclude the period immediately surrounding the disaster to avoid including injuries from the disaster. This also serves to ensure that the choice environment resembles the pre-period as much as possible. We provide more on the rationale for our time-periods in Appendix B.[4]

Location	Month/Year	Severe Weather	Hospital(s) Closed
Northridge, CA	Jan-94	Earthquake	St. John's Hospital
Americus, GA	Mar-07	Tornado	Sumter Regional Hospital
New York, NY	Oct-12	Superstorm Sandy	NYU Langone
			Bellevue Hospital Center
			Coney Island Hospital
Moore, OK	May-13	Tornado	Moore Medical Center

(a) Disaster Details

Hospital	Closure Date	Pre-Period	Post-Period	Partial Reopen	Full Reopen
St. John's	1/17/94	1/92 to 1/94	5/94 to 9/94	10/3/94	10/3/94
Sumter	3/1/07	1/06 to 2/07	4/07 to 3/08	4/1/08	4/1/08
NYU	10/29/12	1/12 to 9/12	11/12 to 12/12	12/27/12	4/24/14
Bellevue	10/31/12	1/12 to 9/12	11/12 to 12/12	2/7/13	2/7/13
Coney	10/29/12	1/12 to 9/12	11/12 to 12/12	2/20/13	6/11/13
Moore	5/20/13	1/12 to 4/13	6/13 to 12/13	5/16	5/16

(b) Pre and Post Periods

Table I Natural Disaster Details and Dates

For our research design, we require that the disaster did not meaningfully disrupt the wider area beyond closing particular hospitals. In that case, we might worry that predictions based on the pre-period would not be meaningful following the disaster. For the six hospitals we focus on in this paper, our analysis suggests that the extent of the damage was limited compared to the size of the affected hospitals' service areas.

For example, the green line in Figure 1 shows the path of the tornado that destroyed Sumter Regional Hospital. Its path was very narrow, cutting through Americus city without

[4]Except for St John's, the omitted period is just the month of the disaster. For St. John's, we omit data until the freeway going through Santa Monica was reopened.

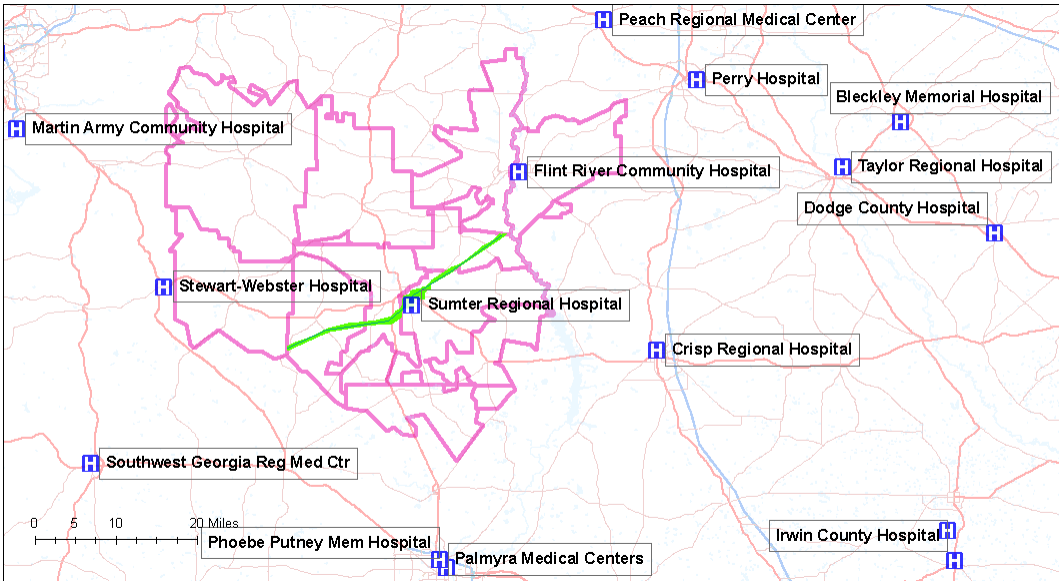

Figure 1 Damage Map in Americus, GA

Note: The green area indicates the damage path of the tornado. The zip codes included in the service area are outlined in pink. Sources: City of Americus, GA Discharge Data

affecting the rural areas surrounding Americus. The tornado in Moore, OK had a similar effect for the city of Moore relative to its suburbs. For Superstorm Sandy, storm damage was mostly limited to areas adjacent to the East River or Long Island Sound. Seismic damage from the Northridge Earthquake was more scattered, with much more damage in Santa Monica than neighboring areas. We provide details for all the disasters, including maps, in Appendix A.

Overall, the evidence suggests that the disasters' effect on the relative desirability of different hospitals can be mostly limited to the exclusion of the destroyed hospital from patient's choice sets. Nevertheless, there were some changes to the patient population or providers in the affected areas following the disasters. We examine whether such changes could explain our results in Section 5 and Section 6, as well as in Appendix E.

3.2 Data Sources and Variables

We rely on several sources of data in our analysis. For patient information, we use detailed discharge data collected by the departments of health for the states where disasters took place.[5] For each state, the discharge datasets provide a census of all inpatient episodes for each licensed hospital located within the state; an inpatient episode is defined as a patient admitted to the hospital where the visit lasted at least 24 hours. For each admission, the data provide the date of admission and discharge, patient's zip code of residence, diagnosis on admission, and a variety of demographic characteristics, including age and sex. In addition, we can construct the DRG weight, a commonly used measure of disease acuity developed by Medicare, based on available diagnosis and procedure codes. An important variable is patients' travel time to hospitals; we use ArcGIS to calculate the travel time, including traffic, between the centroid of the patient's zip code of residence and each hospital's address.

We obtain hospital characteristics from the annual American Hospital Association (AHA) Guide and Medicare Cost Reports. These data include such details as for-profit status, whether or not a hospital is an academic medical center or a children's hospital, the number of beds, the ratio of nurses to beds, the presence of different hospital services such as an MRI, trauma center, or cardiac intensive care unit, and the number of residents per bed.[6]

[5]Background details on these data sets are available at the websites of the New York (https://www.health.ny.gov/statistics/sparcs/), Georgia (https://www.gha.org/GDDS), Oklahoma (https://www.ok.gov/health/Data_and_Statistics/Center_For_Health_Statistics/Health_Care_Information/Hospital_Discharge_&_Outpatient_ASC_Surgery_Data/index.html), and California (https://oshpd.ca.gov/data-and-reports/healthcare-utilization/inpatient/) state health departments.

[6]For a few hospitals in California, New York and Oklahoma, the AHA and Medicare Cost Reports only contain data on the total hospital system rather than individual hospitals. For the AHA Guide, see http://www.ahadataviewer.com/book-cd-products/AHA-Guide/. For the Medicare Cost Reports, see http://www.cms.gov/Research-Statistics-Data-and-Systems/Files-for-Order/CostReports/index.html?redirect=/costreports/.

3.3 Affected Patients and Hospitals

In order to identify the set of patients and hospitals affected by the loss of the destroyed hospital, we first identify patients whose choice set was affected by a disaster. All of our destroyed facilities are general acute care (GAC) hospitals; therefore, we exclude patients going to specialty (e.g., long-term care or psychiatric) hospitals. Such facilities are primarily focused on treating patients with different diagnoses and conditions than the destroyed hospitals. We also exclude patients who do not have, or are unlikely to have had, autonomy in their hospital choice, such as newborns and court ordered admissions, as well as patients who are likely to consider a broader set of hospitals than just general acute care hospitals given their condition, such as those with psychiatric or eye issues.[7]

We then construct the 90% service area for each destroyed hospital using the discharge data, which we define as the smallest set of zip codes that accounts for at least 90% of the hospital's admissions. Because this set may include areas where the hospital is not a major competitor, we exclude any zip code where the hospital's share in the pre-disaster period is below 4%. Our approach assumes that any individual that lived in this service area and required care at a general acute care hospital would have considered the destroyed hospital as a possible choice.

Having established the set of patients affected by the loss of a choice, we turn to defining

[7]We drop newborns, transfers, and court-ordered admissions. Newborns do not decide which hospital to be born in (admissions of their mothers, who do, are included in the dataset). Similarly, government officials or physicians, and not patients, may decide hospitals for court-ordered admissions and transfers. We drop diseases of the eye, psychological diseases, and rehabilitation based on Major Diagnostic Category (MDC) codes, as patients with these diseases may have other options for treatment beyond general hospitals. We also drop patients whose MDC code is uncategorized (0), and neo-natal patients above age one. We also exclude patients who are missing gender or an indicator for whether the admission is for a Medical Diagnosis Related Group (DRG).

the set of relevant substitute hospitals. We identify these as any general acute care hospital that has a share of more than 1% of the patients in the 90% service area, as defined above, in a given month (quarter for the smaller Sumter and Moore datasets) prior to the disaster. We combine all general acute care hospitals not meeting this threshold into an "outside option."

3.4 Descriptive Statistics

Table II displays some characteristics of each destroyed hospital's market environment, including the number of admissions before and after the disaster, the share of the service area that went to the destroyed hospital prior to the disaster, the share of the population that went to the "outside option" prior to the disaster, the number of zipcodes in the service area, and the number of rival hospitals. We also show the average acuity of patients choosing the destroyed hospital during the pre-disaster period as measured by average DRG weight.[8] DRG weights are designed to reflect the resource intensity of patients' treatments. Therefore, differences in the average weights across hospitals reflect variation in treatment complexity.

Table II indicates that Sumter Regional's service area likely experienced a massive change from the disaster; the share of the destroyed hospital in the service area was over 50 percent. For the other disasters, the disruption was smaller though still substantial as the share of the destroyed hospital in the service area ranges from 9 to 18 percent. Thus, patients' choice environments are likely to have changed substantially after the disaster.

Table II also shows that we have a substantial number of patient admissions before and

[8]In this article, when we use the term "DRG weight", we mean the DRG weight used by the Centers for Medicare and Medicaid Services. Since 2007, these are officially called MS-DRG weights.

after each disaster with which to parameterize and test the different models. The number of admissions in the pre-period and post-period datasets ranges from the thousands for Moore and Sumter to tens of thousands for the New York hospitals and St. John's.[9]

Table II Descriptive Statistics of Affected Hospital Service Areas

	Pre-Period Admissions	Post-Period Admissions	Zip Codes	Choice Set Size	Outside Option Share	Destroyed Share	Destroyed Acuity
Sumter	6,940	5,092	11	15	3.6	50.4	1.02
StJohns	97,030	18,130	29	21	9.1	17.4	1.30
NYU	79,950	16,696	38	19	11.0	9.0	1.40
Moore	9,763	3,920	5	12	1.8	11.0	0.93
Coney	46,588	9,666	8	17	7.4	18.2	1.16
Bellevue	46,260	9,152	19	20	8.0	10.8	1.19

Note: The first column indicates the number of admissions in the pre-period data, the second column the number of admissions in the post-period data, the third column the number of zip codes in the service area, the fourth column the number of choices (including the outside option), the fifth column the share of admissions in the pre-period from the 90% service area that went to the outside option, the sixth column the share of admissions in the pre-period from the 90% service area that went to the destroyed hospital, and the seventh column the average DRG weight of admissions to the destroyed hospital in the pre-period data.

4 Estimation

Most models of hospital demand (e.g., Capps et al., 2003; Ho, 2006; Gaynor et al., 2013; Gowrisankaran et al., 2015; Ho and Lee, 2019) use similar parameterizations for patient preferences. In particular, they assume that patient i's utility for hospital j is given by:

$$u_{ij} = \delta_{ij} + \epsilon_{ij}, \tag{1}$$

[9]The New York service areas do overlap. The service area for NYU is much larger than Bellevue, so most of the zip codes for Bellevue are also in the service area for NYU, but the reverse is not true. NYU has a 3.9 percent share in the Coney service area and 9.5 percent share in the Bellevue service area, and Bellevue has a 5.7 percent share in the NYU service area.

where ϵ_{ij} is distributed type I extreme value (logit). The patient has a choice set of J hospitals. The logit assumption implies that the probability that patient i receives care at hospital j is:

$$s_{ij} = \frac{\exp(\delta_{ij})}{\sum_{k \in J} \exp(\delta_{ik})}. \tag{2}$$

Given (2), in the event that hospital j is removed from i's choice set, the likelihood that i chooses to receive care at k – as opposed to other hospitals in J – will be:

$$D_i^{jk} = \frac{\exp(\delta_{ik})}{1 - \exp(\delta_{ij})}. \tag{3}$$

Here, D_i^{jk} represents the choice removal diversion ratio from j to k for patient i. Constructing the overall population's choice removal diversion ratio for j to k involves averaging across the D_i^{jk}'s for all patients i in the market. We denote this overall choice removal diversion ratio D^{jk}. This calculation presumes that patients would not continue seeking treatment from j after it disappears from J.

4.1 Model Parameterizations

While the previous literature estimating hospital demand has typically assumed a logit error as in (2), researchers have specified the parametric component of utility δ_{ij} differently. The following parameterization encompasses the different models used in the literature:

$$\delta_{ij} = \sum_m \sum_l \beta_{ml} x_{jm} z_{il} + \gamma \sum_l z_{il} \alpha_j + \sum_m \sum_l f(d_{ij}; x_{jm} z_{il}) + \alpha_j, \tag{4}$$

where i indexes the patient, j indexes the hospital, l indexes patient characteristics, and m indexes hospital characteristics. Then, z_{il} are patient characteristics (such as patient age and diagnosis), x_{jm} are hospital characteristics (such as number of nurses per bed), α_j are alternative specific constants in the language of McFadden et al. (1977), and d_{ij} is the travel time between the patient's zip code and the hospital. The function $f(d_{ij}; x_{jm} z_{il})$ represents distance interacted with hospital and patient characteristics.

Thus, the first term represents interactions between patient characteristics and hospital characteristics, the second term interactions between patient characteristics and hospital indicators, the third term some function of distance interacted with patient and/or hospital characteristics, and the fourth term α_j alternative specific constants. We summarize the differences between these models in Table III; Appendix H lists the variables present in each model. Since we do not have price information in our datasets and most patients do not pay out-of-pocket for differences between hospitals, we follow (Ho, 2006, 2009) in not including price as a covariate; Gaynor et al. (2013) have shown that omitting prices does not materially affect predictions.

Our first and simplest model, *AggShare*, relies exclusively on a set of alternative specific constants α_j to model δ. In other words, all patients within the relevant area have, up to the logit shock, the same preferences for each hospital. In this framework, patient choice probabilities are proportional to observed aggregate market shares and can be estimated with aggregate data.

The most important differentiator among models that allow for patient-level heterogeneity is whether or not they assume that patients' choices can be modeled exclusively in "characteristics" space (Lancaster, 1966; Aguirregabiria, 2011). We consider two models,

CDS and *Char*, that model δ using just interactions between patient attributes (age, sex, income, condition, diagnosis) and hospital characteristics (for-profit status, teaching hospital, nursing intensity, presence of delivery room, etc.) and several interactions between patient characteristics and travel time. They differ in which patient and hospital characteristics they include as covariates. In both models, γ and α_j are set to zero. *CDS* is based on Capps et al. (2003), while *Char* is based on one of the models in Garmon (2017).

Four models include alternative specific constants α_j and functions thereof $z_{il}\alpha_j$ in addition to some measures of patient-level heterogeneity. These models differ in their sets of included variables other than the hospital indicators. The first model, *Time*, is based on May (2013), and just includes a set of hospital indicators, travel time, and travel time squared. The second model, *Ho*, is based on Ho (2006), and includes α_j and interactions between hospital characteristics and patient characteristics, so β_{il} is non zero. However, it excludes interactions with hospital indicators, so γ is always zero. The third model, *GNT*, is based on Gowrisankaran et al. (2015), and includes a large set of interactions between travel time and patient characteristics. However, it only includes a small number of interactions of hospital indicators and hospital characteristics with patient characteristics. Finally, we consider a fourth model, *Inter*, that includes interactions of hospital indicators with acuity, major diagnostic category, and travel time as well as interactions between patient characteristics and travel time.

Our final model, *Semipar*, is a semiparametric bin estimator similar to that outlined in Raval et al. (2017), and does not use data on hospital characteristics. This estimator models hospitals in product space, and estimates alternative specific constants for each group. Formally,

$$s_j^g = \frac{e^{\delta_j^g}}{\sum_{j' \in J} e^{\delta_{j'}^g}}.$$

Using this approach, we can compute the choice removal diversion ratios using the estimated $\hat{\delta_j}^g$. In our implementation, all patients are assigned a group based upon their zip code, disease acuity (DRG weight), age group, and area of diagnosis (MDC). More details on our implementation of this estimator are in Appendix C.

Table III Summary of Tested Models

Model	Spatial Differentiation	Hospital Quality	Patient Interactions
AggShare	No	Indicators	No
Char (Garmon, 2017)	Travel Time	Characteristics	Yes
CDS (Capps et al., 2003)	Travel Time	Characteristics	Yes
Time (May, 2013)	Travel Time	Indicators	No
Ho (Ho, 2006)	Travel Time	Both	Yes
GNT (Gowrisankaran et al., 2015)	Travel Time	Both	Yes
Inter	Travel Time	Indicators	Yes
Semipar (Raval et al., 2017)	Zipcode (Groups)	Indicators	Yes (Groups)

Note: Each row is a stylized depiction of a given model. The first column gives the model "name" we use in the paper and the citation (if applicable), the second column how the model incorporates spatial differentiation, the third column how the model incorporates differing hospital quality (through hospital characteristics, indicators, or both), and the fourth column whether the model incorporates interactions with patient characteristics, which may include race, sex, and age, as well as the different diagnoses and procedures they have and their relative severity.

4.2 Diversion Ratios

Because the logit implies individual level proportional substitution to all other choices when a given choice is removed from the choice set, the choice probabilities are sufficient to compute

diversion ratios. Thus, for each model, we can estimate diversion ratios by using the models' predicted choice probabilities.

Under these assumptions, the predicted (aggregate) diversion ratio from the destroyed hospital j to non-destroyed hospital k is:

$$\hat{D}^{jk} = \sum_i \underbrace{\frac{\hat{s}_{ik}}{1-\hat{s}_{ij}}}_{D^{ijk}} \underbrace{\frac{\hat{s}_{ij}}{\sum_i \hat{s}_{ij}}}_{w_{ij}}, \tag{5}$$

where $\hat{s}_{ij}$ is the predicted probability that patient i chooses to go to hospital j. The aggregate diversion ratio D^{jk} is thus a weighted average of the patient level diversion ratios D^{ijk}. The weights, w_{ij}, are given by each patient i's expected share of overall hospital admissions at the destroyed hospital. All of these choice probabilities are estimated on data from the pre-period, as would be done in a prospective merger analysis.

Because we observe patient choices post-disaster, we can also compute the *observed* aggregate diversion ratio for hospital k as the share of hospital j's patients that hospital k captured following the destruction of hospital j. In other words,

$$D^{jk}_{\text{observed}} = \frac{s_k^{\text{post}} - s_k^{\text{pre}}}{s_j^{\text{pre}}}, \tag{6}$$

where s_k^{post} is the post merger share of hospital k, s_k^{pre} is the pre-merger share of hospital k, and s_j^{pre} is the pre-merger share of the destroyed hospital. These shares are all computed based upon the full patient population in each period.

As we describe in Section 5, we compare the predicted diversion ratios from the models estimated on the pre-period data ($\hat{D}^{jk}$) to the observed diversion ratios following the natural

disaster (D^{jk}_{observed}). Ideally, we need the choice environments to be identical except for the elimination of the destroyed hospital. In particular, we want that:

1. The distribution of preferences over facilities in the post-disaster period is identical to the pre-disaster distribution,

2. The types of patients going to the hospital do not change, and

3. The characteristics of non-destroyed hospitals do not change.

Given these conditions, the observed diversion ratio calculated using the variation in choice sets caused by the disaster is an unbiased estimate of the true diversion ratio. We compare this unbiased estimate to those derived from our logit choice models estimated on pre-disaster data. We examine whether violations of these conditions explain our findings in Section 6.

4.3 Implementation

We estimate all of the models separately for each experiment. For all of the models except *Semipar*, we use maximum likelihood for estimation on patient-level discharge data from the pre-disaster period. We report details of our model estimates for these models, including the number of parameters in the model, the estimated log likelihood of the model, the AIC and BIC criteria, and McFadden's pseudo R^2, in Appendix D. *Inter* minimizes the AIC criterion for five of the six experiments and the BIC criterion for three of the six experiments. *Ho* minimizes the AIC criterion for Bellevue and the BIC criterion for Bellevue and Coney. *GNT* minimizes the BIC criterion for Sumter. For *Semipar*, we employ the algorithm described in Appendix C to estimate choice probabilities on patient-level discharge data from the pre-disaster period.

Given model estimates of choice probabilities, we can predict diversion ratios from the destroyed hospital to all other hospitals using (5). We also recover observed diversion ratios with (6) using the pre-period and post-period data. For the New York hospitals, our predicted and observed diversion ratios are based on all hospitals in the choice set taken out of service due to the disaster.

To compute standard errors, we take into account sampling variation in both the pre-period, where it will affect both observed diversion ratios and predicted diversion ratios through model estimates of choice probabilities, and in the post-period data, where it will just affect observed diversion ratios. We account for sampling variation through 200 bootstrap replications of the pre-period data and post-period data; we re-estimate all the models and recalculate both model predicted and observed choice removal diversion ratios on these bootstrap samples. We use the bootstrap estimates to bias correct our estimates and compute 95% confidence intervals.[10]

5 Predictive Performance

Across all of the experiments, we estimate 94 choice removal diversion ratios from the destroyed hospitals to others in patients' choice sets, including the outside option. We quantify the quality of model predictions using the prediction error, which we define as $\hat{D}^{jk} - D^{jk}_{\text{observed}}$. For example, if the predicted choice removal diversion ratio for a hospital

[10]For two models, diversion estimates could not be calculated for every individual for some of the bootstrap samples of the Sumter disaster. These issues arise for the *Semipar* model because for some set of individuals the probability of going to the destroyed hospital is one in the bootstrap samples, and for the *Ho* model owing to a particular interaction term being inestimable. For both models, the number of such circumstances is small, with the average number of admissions with a missing diversion between 7 and 12. We exclude individuals for whom diversions can not be calculated from our estimates for these bootstrap samples.

was 15%, and the observed post-disaster diversion ratio 20%, then the prediction error would be -5%.

We then compare the prediction error to the observed diversion ratio for the *Semipar* model in Figure 2a. Using the linear best fit line, the prediction error is -5% when the observed diversion ratio is 20%. The slope of the linear best fit line is -0.35, so a one percentage point increase in observed diversion ratio is associated with an average 0.35 percentage point decrease in the prediction error for the *Semipar* model. Thus, we tend to substantially underpredict large observed diversion ratios.

One potential explanation for these findings is that the composition of patients changes after the disaster because patients defer treatment following the disaster. All else equal, one might think that such deferrals would be more pronounced for elective procedures, rather than urgent or emergency admissions. If such patients have consistently different tastes, such as a greater disutility from travel, then this might produce results akin to those we find.

To address this possibility, we re-estimate all of the models using only non-elective admissions. We then examine the predictive performance of our models for non-elective admissions before and after the disaster.[11] Figure 2b presents the analogue to Figure 2a for the non-elective sample. It shows similar patterns to those for the full sample. The slope coefficient on the best fit line is -0.43 for the *Semipar* model for the non-elective sample, compared to -0.35 for the full sample, so the models perform *worse* on the non-elective sample.[12]

We now focus the remainder of our analysis on the non-elective sample. We present the full sample analogues of all figures and tables in Appendix F and Appendix G. In addition, to

[11] We define non-elective admissions as admissions coded as "Emergency" or "Urgent" in the admission type variable or coded as a labor and delivery, either through the admission type variable (if applicable) or a Major Diagnostic Category (MDC) of 14.

[12] Descriptive statistics for the sample of non-elective patients is presented in Table A-1 in Appendix G.

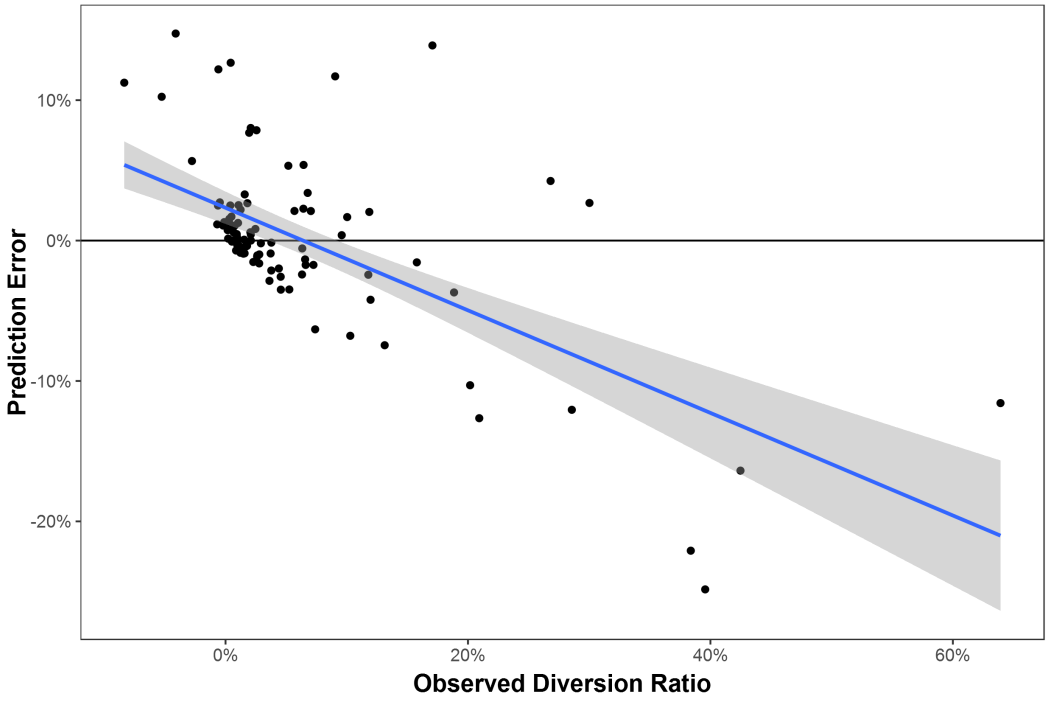

(a) Full Sample

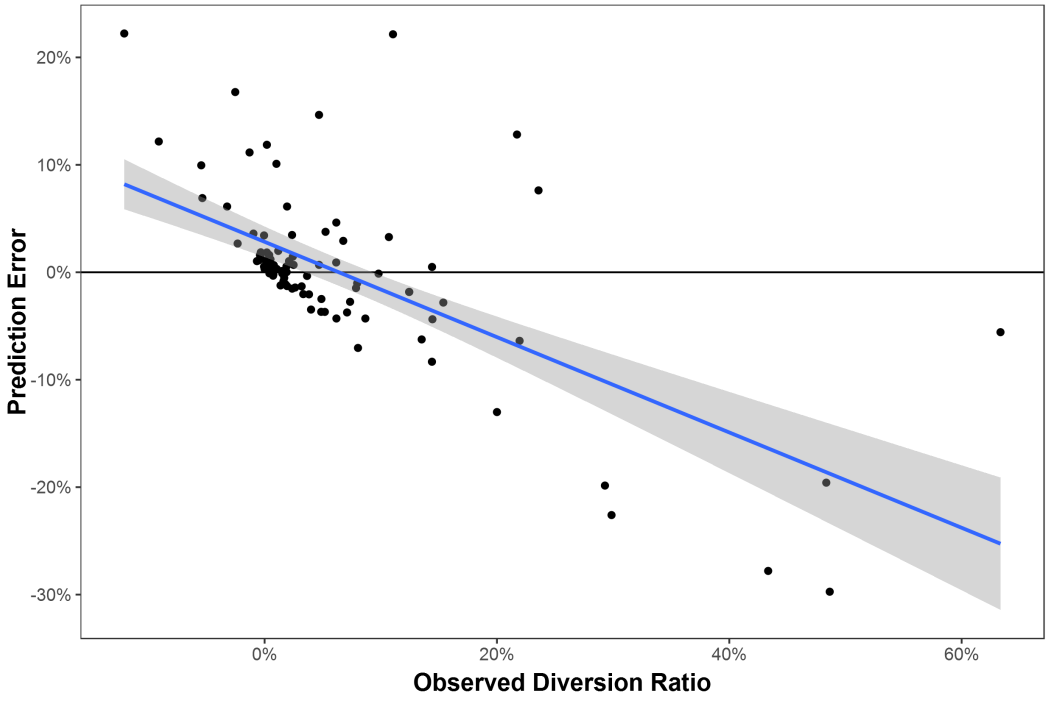

(b) Non Elective Sample

Figure 2 Prediction Error By Observed Choice Removal Diversion Ratio

Note: Each point represents the diversion ratio to a hospital from one of the six experiments. The blue line is the linear regression line through the points, and the grey shading the 95% confidence interval for the linear regression line. The left figure contains the results for the full sample and the right figure contains the results for the non-elective sample.

compare across models and disasters, we focus on the slope of the best fit line in a regression of the prediction error on observed diversion ratios:

$$\frac{Cov(\hat{D}^{jk} - D^{jk}_{\text{observed}}, D^{jk}_{\text{observed}})}{Var(D^{jk}_{\text{observed}})} \tag{7}$$

The slope directly connects to Figure 2 as it is the slope of the blue best fit line, and is negative if larger observed diversion ratios imply greater underprediction of the diversion ratio as it grows larger. Given that diversion ratios sum to one, the intercept of the best fit line is a function of the slope parameter, so the slope shows the degree of bias in the estimates.[13]

We depict this slope for each experiment for the *Semipar* model in Figure 3a. The finding that we consistently underpredict large diversion ratios is not being driven by particularly poor predictive performance in one disaster. The slope coefficient is between -0.5 and -0.75 for four disasters, and we can reject that the slope is equal to zero for all disasters but Bellevue.

Figure 3b demonstrates that we underpredict high diversion ratio hospitals in all of the models we estimate. However, the models can be divided into two groups in terms of their accuracy. The aggregate share model, and the two models that do not include alternative specific constants, *Char* and *CDS*, have slope coefficients of around -0.6, so a 10 percentage point increase in the observed diversion ratio decreases the prediction error by

[13]The y intercept in the regression of the prediction error on observed diversion ratios is equal to $\frac{-\beta_1 T}{N}$, where T is the number of experiments, N is the total number of hospitals across all experiments, and β_1 the slope coefficient as above. To see this, consider that we model $D^{predicted}_{kt} - D^{observed}_{kt} = \beta^0 + \beta^1 D^{observed}_{kt} + \epsilon_{kt}$, where k indexes hospitals and t markets. Since within each market the sum of both the predicted and observed diversion ratios must sum to one and $\sum_k \hat{\epsilon}_k = 0$, we have $0 = N\hat{\beta}_0 + T\hat{\beta}_1$, where the hat denotes an estimated value. Then solving for β_0 yields the expression above.

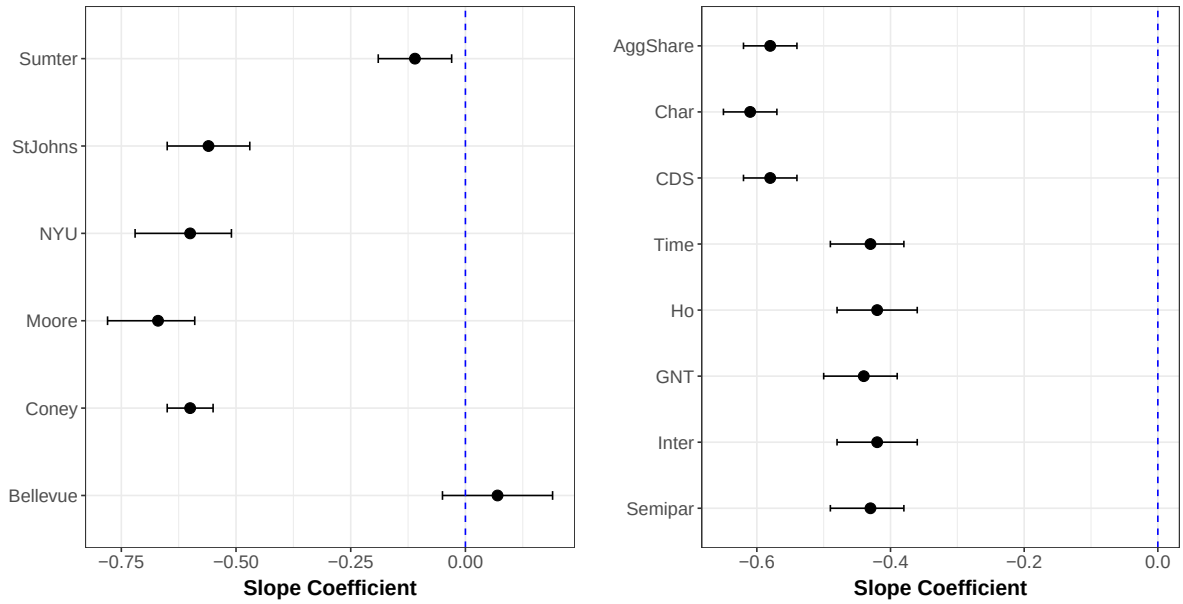

(a) By Experiment (for *Semipar*) (b) By Model

Figure 3 Slope Coefficient of Observed Choice Removal Diversion Ratios on Prediction Error, Non-Elective Sample

Note: The left figure depicts the slope of the observed diversion ratio on the prediction error by experiment for the *Semipar* model, while the right figure depicts the same by model. Bars represent 95% confidence intervals computed from 200 bootstrap replications; we also apply a bootstrap bias correction. See Table A-2 and Table A-3 for tables of the estimates and confidence intervals used to generate these figures.

6 percentage points. By contrast, models that use the individual level data to allow spatial differentiation, and also allow unobserved vertical quality via alternative specific constants have slope coefficients of slightly under -0.4 on average. That is, the magnitude of the slope coefficient declines by 25 to 30 percent when accounting for these two features of demand in the model.

To understand what may be driving the differences across models, we decompose the choice removal diversion ratio from hospital j to hospital k (D^{jk}) into two components[14]:

$$D^{jk} = \sum_i D^{ijk} \frac{s_{ij}}{\sum_i s_{ij}} = \underbrace{E[D^{ijk}]}_{Individual} + \underbrace{\frac{Cov(D^{ijk}, s_{ij})}{E(s_{ij})}}_{Heterogeneity\ \ Factor} . \tag{8}$$

The first term is the average individual level (indexed by i) choice removal diversion ratio in the data. The second term, which we call the "heterogeneity factor", increases when patients with a larger probability of going to the destroyed hospital j also have a larger probability of going to hospital k.

In Figure 4, we depict the slope coefficient of the observed diversion ratio on the prediction error after either including the heterogeneity factor in the predicted diversion in red, or excluding it in blue. The models that perform badly do so for different reasons. The magnitude of the slope coefficient for *AggShare* excluding the heterogeneity factor is smaller than for *CDS* and *Char*. However, its heterogeneity factor is zero since it does not allow for

[14]The derivation is below:

$$\begin{aligned} D^{jk} &= \sum_i D^{ijk} \frac{s_{ij}}{\sum_i s_{ij}} = \frac{1}{N} \sum_i D^{ijk} + \sum_i D^{ijk} (\frac{s_{ij}}{\sum_i s_{ij}} - \frac{1}{N}) = \frac{1}{N} \sum_i D^{ijk} + \frac{\sum_i D^{ijk} (s_{ij} - \frac{1}{N} \sum_i s_{ij})}{\frac{1}{N} \sum_i s_{ij}} \\ &= E_i[D^{ijk}] + \frac{Cov_i(D^{ijk}, s_{ij})}{E_i(s_{ij})} \end{aligned}$$

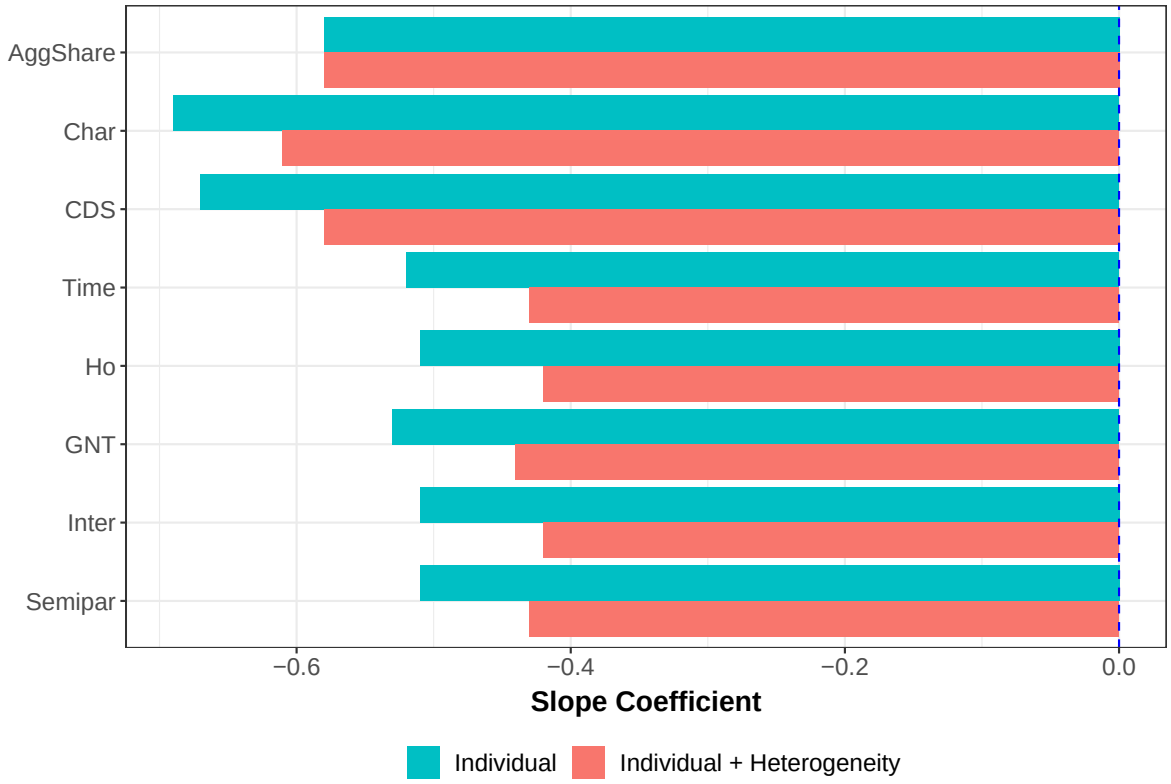

Figure 4 Decomposition of Average Predicted Diversion, Non-Elective Sample

Note: We report the slope coefficient of the observed diversion ratio on the prediction error based upon the average individual diversion ratio in blue, and based upon the individual diversion ratio plus the heterogeneity factor (i.e. the total predicted diversion) in red, for each model. Each term is as defined in the text. See Table A-4 for a table of the estimates and confidence intervals used to generate this figure and Figure A-2 and Table A-12 for the equivalent figure and table for the full sample.

any heterogeneity in choice probabilities.

For the *CDS* and *Char* models, the decrease in magnitude of the slope coefficient due to the heterogeneity factor is similar to the models that perform well. However, the magnitude of the slope coefficient based on the prediction error using just the expected individual diversion ratio is much greater than the other models. Therefore, these models perform poorly for different reasons – the aggregate share model does not allow for horizontal differentiation, while *CDS* and *Char* are worse at estimating vertical quality because they do not allow for alternative specific constants.

In addition, all of the models that include alternative specific constants and controls for patient location – *Time*, *Ho*, *GNT*, *Inter*, and *Semipar* – have similar values of the slope coefficient including, and excluding, the heterogeneity factor. This similar performance is despite the fact that they vary substantially in the degree of heterogeneity they allow across different types of patients. For example, *Time* allows no heterogeneity in preferences over vertical quality or travel time across patients, while *Semipar* allows preferences to vary in an unrestricted fashion across many narrowly defined groups. This similarity suggests that allowing greater heterogeneity on observed patient characteristics does not consistently improve estimates of diversion ratios.

6 Mechanisms

We now examine why all of the models underpredict large diversion ratios. First, we show that we underpredict diversion to nearby hospitals and overpredict diversion to the outside option. One explanation for this is unobserved heterogeneity in the disutility for travel. We

then estimate random coefficient models that allow such unobserved heterogeneity, and find significant improvements in model performance. Second, we examine the effects of potential changes to physician labor supply due to the disaster. Finally, we consider a number of other potential explanations, and find evidence against explanations due to capacity constraints and changes in patient composition.

6.1 Preference Heterogeneity in Travel Time

The average prediction error increases with the average distance of a hospital to patients in the service area. Figure 5a replicates Figure 2b, except with average travel time expressed as a percentage of the market average travel time on the X axis. Because the hospitals grouped in the outside option are typically located farther away than the other choices, we assign the outside option hospitals (shown in red on the figure) the maximum travel time of any choice in the choice set.

Figure 5a shows that the *Semipar* model underpredicts diversion to hospitals with less than the average travel time, and overpredicts diversion to more distant hospitals and, especially, the outside option. Figure 5b depicts the average prediction error for each model for hospitals that are below the average distance, above the average distance, or either above the average distance or the outside option. For the *Semipar* model, the average prediction error is -1.2 percentage points for hospitals in the choice set less than the average travel time away from the destroyed hospital. By contrast, the average prediction error is 0.1 percentage points for hospitals more than the mean time away, and 0.86 percentage points for hospitals more than the mean time away or the outside option. For only the outside option, the

average prediction error is a full 7.4 percentage points!

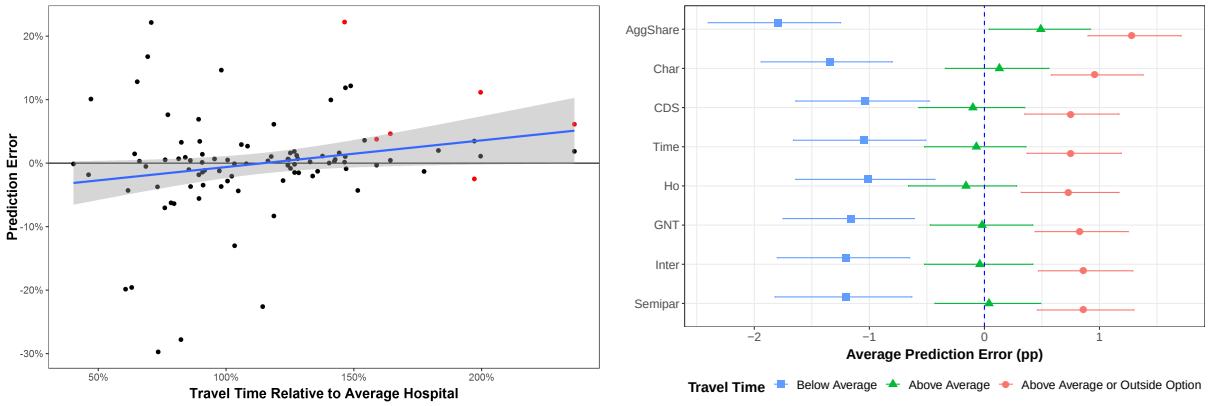

(a) By Model (b) Average Prediction Error by Distance Group

Figure 5 Prediction as a Function of Distance, Non-Elective Sample

Note: First panel shows the prediction error as a function of the average travel time to the hospital expressed as a percent of the average travel time in the market. Second panel presents the average prediction error, differentiating between hospitals whose travel time is below average for their market, above average for their market, or above average plus the Outside Option. Bars represent 95% confidence intervals computed from 200 bootstrap replications; we also apply a bootstrap bias correction. See Table A-5 for tables of the estimates and confidence intervals used to generate these figures.

Observed Consumer Heterogeneity The estimates above showed that we underpredict diversion to nearby hospitals and substantially overpredict the outside option. One explanation for these results is that the models we estimate are missing interactions between travel time and components of consumer heterogeneity.

Many of the models we estimate allow for both the effects of patient location and hospital quality to vary by patient characteristics, including diagnosis, race, gender, and age. In Figure 6.1, we show that interactions with such characteristics do improve predictions of individual patients' choices. We measure the quality of patients' choice predictions by the share of individual predictions that are correctly predicted, in that the patient goes to the hospital predicted to be most likely by the econometric model. In general, models allowing

more individual heterogeneity do a better job predicting patients' choices.

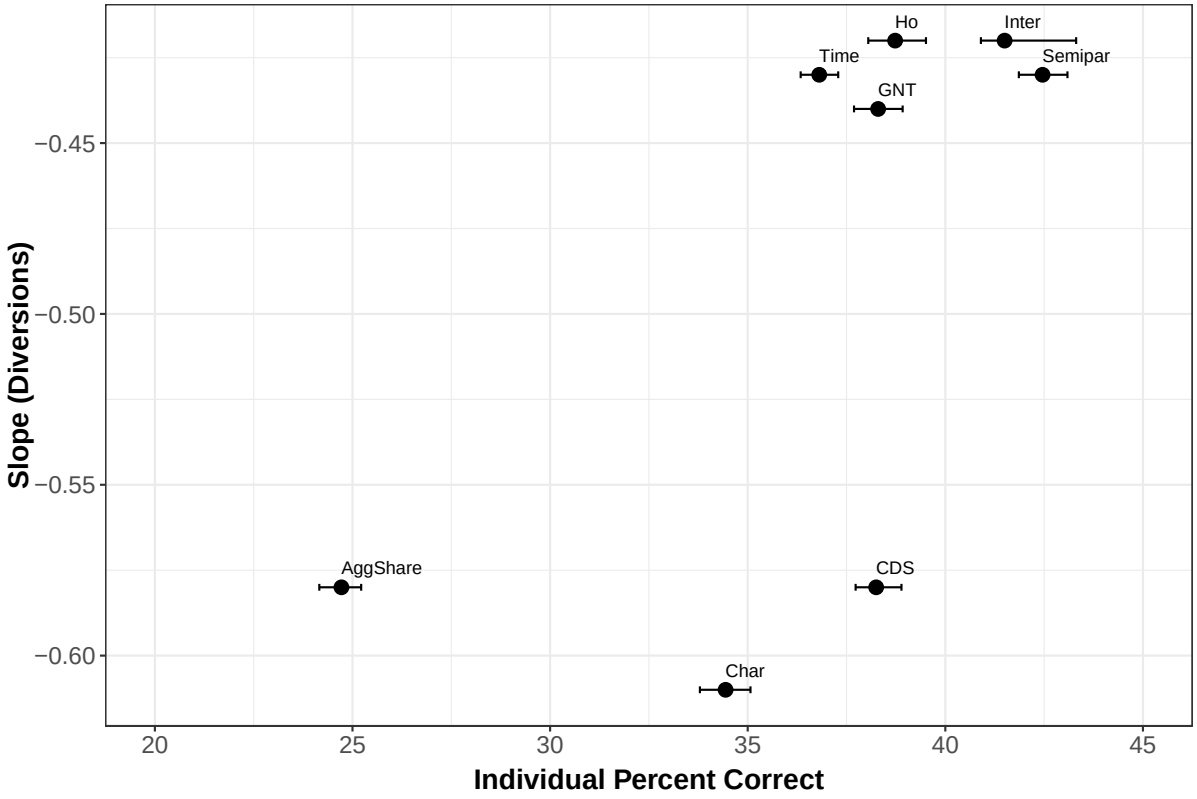

Figure 6 Average Percent Correct of Individual Predictions vs. Slope Coefficient of Observed Diversion Ratio on Prediction Error, Non-Elective Sample

Note: The Figure compares the slope coefficient of the observed diversion ratio on the prediction error to the average percentage of individual choices correctly predicted. Bars represent 95% confidence intervals computed from 200 bootstrap replications; we also apply a bootstrap bias correction. See Table A-2 and Table A-6 for estimates and confidence intervals used to generate the figure.

However, better predictions of individual choices are not associated with better predictions of diversion ratios. For example, while *Semipar* is, on average, the best performing of the models in predicting individual patient choices following the disasters, it has approximately the same slope coefficient as *Time*, which does much worse at predicting patient choices. These results suggest that allowing for preference heterogeneity using observed patient characteristics does not help to predict aggregate diversion ratios.

Unobserved Consumer Heterogeneity Instead, patients may differ in their willingness to travel in ways that our observed characteristics do not capture. Patients who would have gone to the destroyed hospital, and so were forced to switch, could have less willingness to travel than the "average" patient in the service area in the pre-period. In that case, patients who traveled long distances in the pre-disaster period might provide poor comparisons for otherwise observably similar patients in the post-disaster period.

We test the hypothesis that patients have heterogeneous travel costs by estimating a series of random coefficient logit models that allow for a normally distributed random coefficient on travel time. Because of the computational cost, we restrict attention to the simple *Time* model that only includes travel time and hospital specific indicators as explanatory variables. Using this approach, we trace out the post-disaster predictive performance of different standard deviations of the random coefficient on travel time. Implicitly, this approach uses the post-disaster variation to estimate the standard deviation of the random coefficient.

We make a number of modifications to our baseline analytical framework to facilitate estimation of the random coefficient models. First, patients with a greater disutility for travel will likely have a lower utility from the outside option, because patients going to the outside option typically travel further than for the other options. For each disaster, we set the distance of the outside option to the maximum distance from any patient zip code to any hospital in the choice set. In practice, this means we are setting the outside option to zero (as before) but all other choices have their distance and squared distance as $time - max\ time$ and $(time^2 - max\ time^2)$, respectively.

Second, the random coefficient on travel time is a draw from a normal distribution multiplied by the distance coefficient estimate from the model without a random coefficient.

We do this to scale the variance for each disaster in a way that allows for cross-disaster comparisons of the standard deviation of the random coefficient. We estimate the standard deviation of this normal distribution from a grid evenly spaced between 0 and 1.5.

Using the post-disaster data, we compute the mean squared error between predicted and observed diversion ratios for each standard deviation of the random coefficient. In Figure 7, we show the Mean Squared Prediction Error as a function of the standard deviation of the random coefficient. In this figure, the mean squared error is averaged over all of the disasters. Adding the random coefficient improves the models' predictions of diversion ratios.

We use two different approaches to estimate the standard deviation over the grid considered. In the first, *Common SD*, we compute the optimal standard deviation averaging across all experiments (the approach in Figure 7). One concern with this approach is that we overfit the data by adding in the variation of the random coefficient as a free parameter. Therefore, in the second, *LOO SD*, we use a leave one out approach, picking the grid value for a given experiment that minimizes prediction errors for all other experiments. In this implementation, there is no concern of overfitting, since the data set of the estimation differs from that of testing the predictions.

In Figure 8a, we present the slope coefficient between the actual choice removal diversion ratio and the prediction error for the different models. Consistent with the results in Figure 3, we find that, without a random coefficient on travel time, the slope coefficient is -0.43. However, the slope coefficient falls in magnitude to approximately -0.35 for *Common SD* and -0.32 for the *LOO SD* models. In Figure 8b, we compare the random coefficient models to the *Zero SD* model. This graph shows a 20% decline in magnitude of the slope coefficient for *LOO SD* and 25% for *Common SD* relative to *Zero SD*. We can reject the null hypothesis

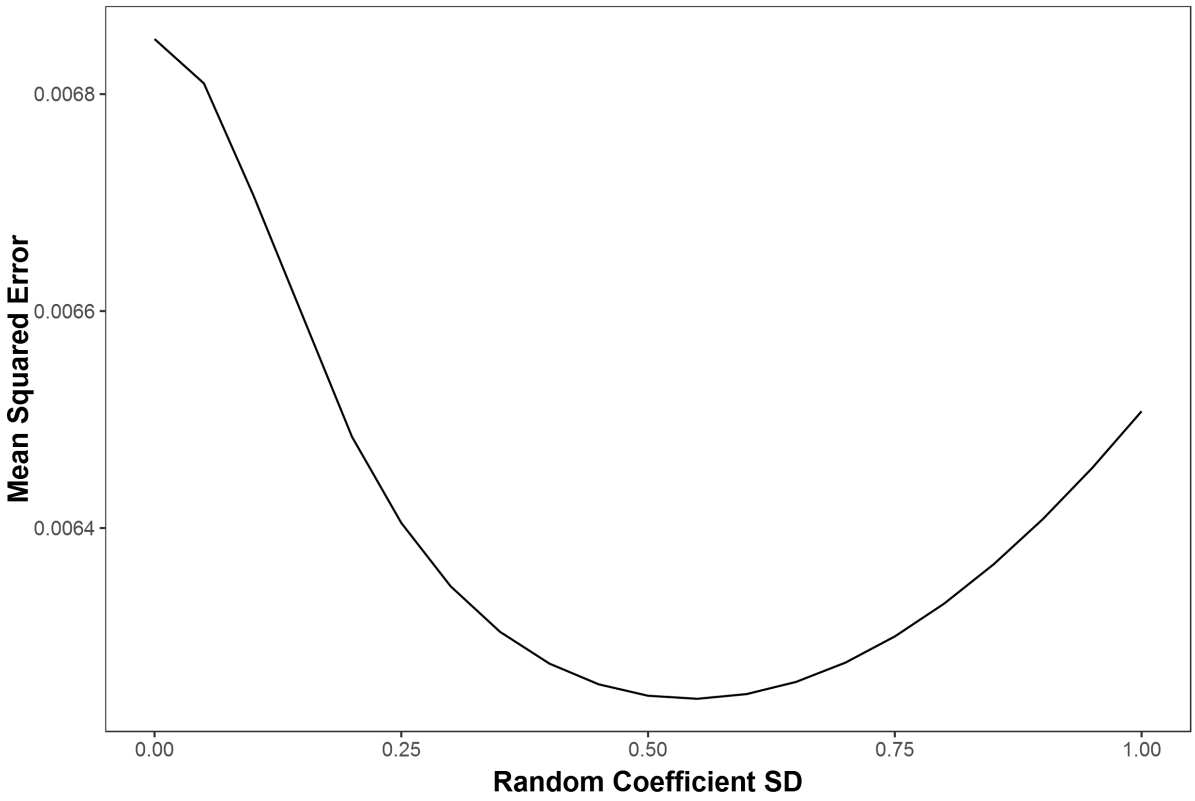

Figure 7 MSE by Standard Deviation of Random Coefficient

Note: This figure shows the mean squared prediction error (MSE) of the *Common SD* class of models described in the text, where the models vary by the standard deviation of the random coefficient.

of no improvement.

Overall, we take these results as evidence that preference heterogeneity in travel time could explain some of the underprediction of diversion to nearby hospitals, and overprediction of diversion to the outside option. More generally, they suggest that allowing for unobserved heterogeneity through random coefficients may lead to better predictions even when economists have access to rich individual level data that allows them to model observed heterogeneity.

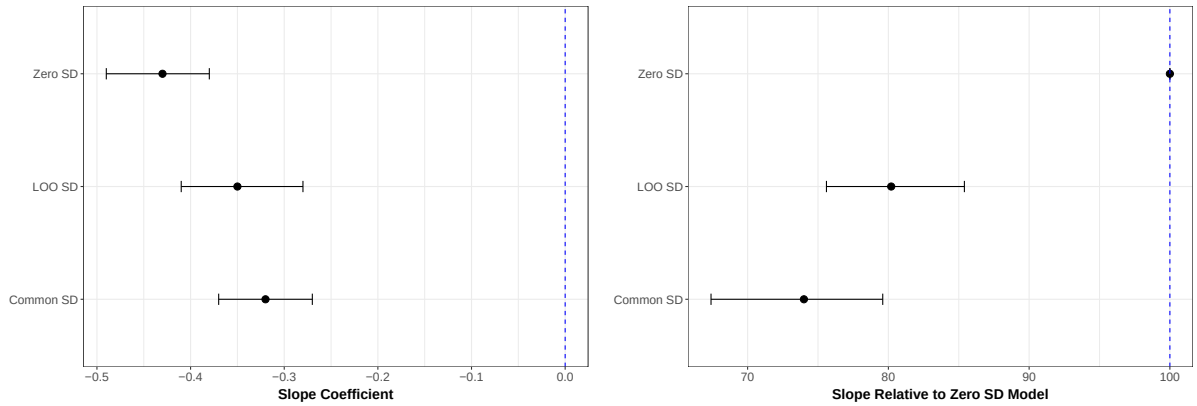

(a) By Model (b) Correlation by Distance

Figure 8 Random Coefficient Relative Performance

Note: The left panel presents the slope of the observed diversion ratio on the prediction error. The right panel depicts the slope for a model relative to that for the Zero SD model. 95% confidence intervals are computed from 200 bootstrap replications; we also apply a bootstrap bias correction. See Table A-9 for estimates and confidence intervals used to generate the figure.

6.2 Physician Labor Supply

Another set of explanations for our findings is the interaction between physician choice and hospital choice. As Ho and Pakes (2014) point out, demand models estimate a "reduced form" referral function that combines patient preferences and physician referral patterns. The model specifications described in Section 4 do not include a role for physician choice, because referring physicians are not observed in most hospital discharge datasets. Physician choice could affect our analysis in three major dimensiosn.

First, even if the disaster does not affect physician labor supply, both Beckert and Collyer (2017) and Raval and Rosenbaum (forthcoming) show that accounting for referral patterns can lead to substantially different substitution patterns between hospitals. The clinicians of patients who went to the destroyed hospital might have different referral patterns than the clinicians of other patients in the service area. Thus, we might underpredict certain

hospitals if the clinicians of patients who went to the destroyed hospital tend to refer to those hospitals.[15]

Another potential explanation for our findings is that physicians switch hospitals or locations post-disaster. If operating physicians at the destroyed hospitals moved to underpredicted hospitals, this could explain our findings. We examine this explanation for the New York hospitals, where we have data on operating physicians both pre- and post-disaster.

We do find evidence that physicians moving to a different hospital may have affected diversion ratios for NYU (albeit not other hospitals). For regular NYU clinicians, 45% of the admissions in the post-disaster period were at Lenox Hill hospital.[16] This is consistent with reports that Lenox Hill actively welcomed NYU physicians to practice there post-disaster.[17] Our models considerably underpredict diversion to Lenox Hill for NYU; *Semipar* predicts a diversion ratio of 7.0% compared to an observed diversion of 20.0%.[18] Lenox Hill is the only large observed diversion ratio for NYU that we underpredict. Notably, we did not find similar patterns for regular Bellevue and Coney Island clinicians.

Third, physicians at the destroyed hospitals might not practice at all until the hospital

[15]We illustrate how referring patterns can distort diversion ratios through the following example in which the referring physician induces the patient's consideration set. Patients are only differentiated by their unobserved referring clinician; pre-disaster 50% go to the destroyed hospital, 15% to hospital A and 35% to hospital B. There are two referring clinicians. Clinician 1, who cares for half of all patients, refers to all hospitals, with shares of 40% to the destroyed hospital, 30% to A, and 30% to B. Clinician 2, who cares for the other half, only includes the destroyed hospital and hospital B in patient consideration sets, with shares of 60% to the destroyed hospital, 0% to A, and 40% to B.

Assuming diversion proportional to share, we would estimate diversions of 30% to A and 70% to B from the destroyed hospital. However, since 40% of the destroyed hospitals patients come from clinician 1 and 60% from clinician 2, the true diversion ratio to A is 0.4*0.5 = 20% and to B is 0.4*0.5 + 0.6*1 = 80%. Thus, the model underpredicts the higher diversion by not accounting for referral patterns.

[16]To maximize observations, we do not limit attention to non-elective admissions for this exercise. However, the same pattern is evident in the non-elective sample.

[17]See https://www.nytimes.com/2012/12/04/nyregion/with-some-hospitals-closed-after-hurricane-sandy-others-overflow.html.

[18]In the overlapping Bellevue service area, *Semipar* predicts a diversion ratio of 6.1% to Lenox Hill compared to an observed diversion of 14.4%. This could, at least in part, reflect the fact that our diversion ratios for New York combine multiple destroyed hospitals.

is rebuilt, forcing patients to switch doctors as well as hospitals. Their new doctors might have substantially different referral patterns than their old doctors, so that demand post-disaster is quite different from demand pre-disaster. We indeed find that the level of total admissions at all hospitals for physicians who were regular doctors at the destroyed hospital fell substantially, by 60% for doctors at NYU, 87% for doctors at Bellevue, and almost 94% for doctors at Coney.[19] If patients switch to doctors located closer to them, and their new doctors also prefer nearby hospitals, we might expect greater diversion to proximate hospitals.

6.3 Additional Explanations

Capacity Constraints Post-merger, if some hospitals faced capacity constraints inhibiting their ability to accommodate all of the patients that wished to receive care, our models would overpredict diversion to them and underpredict diversion to other hospitals. We examine this issue in our different markets using information on the total number of patients admitted and the number of beds. We measure capacity as the number of admitted patients divided by the number of beds, and define a hospital as "capacity constrained" if its capacity is above 90%.[20]

For the most part, we do not see evidence of hospitals facing binding capacity constraints, let alone that the disaster created such problems. No hospitals are capacity constrained

[19] We define a "regular doctor" as one with at least 30 admissions in January through September of 2012.

[20] For the Sumter and St. John's disasters, we have data on the date that each patient was admitted and discharged, and so can explicitly measure capacity for each day. For the Moore and Sandy disasters, we only have data on the month of admission and discharge. We thus calculate monthly capacity as a sum of each patient's length of stay for patients admitted in that month divided by the total number of days in the month. While crude, we compare this capacity measure to true capacity for the hospitals in the choice set for Sumter and find that it is approximately unbiased.

using our capacity utilization measure for Sumter and Moore. For St. John's in California, only one hospital is capacity constrained both before and after the disaster. In New York, however, five hospitals move from never constrained before the disaster to constrained in both months after the disaster. All five are in Coney Island's choice set, two in NYU's, and one in Bellevue's. Contrary to what we would expect if the new capacity constraints drove our results, we underpredict diversion for three of these hospitals and correctly predict diversion for two. Thus, it does not appear that capacity constraints explain our findings.

Strategic Investments Our findings could also be explained by hospitals making strategic investments in quality post-disaster. For example, if competitor hospitals targeted outreach to patients living near the destroyed hospital, such strategic investments might have affected patients' preferences over the options available to them. Since switching costs for hospitals are large (Shepard, 2016; Raval and Rosenbaum, 2018), the destruction of the hospital, by forcing patients to switch, may have incentivized competitors to try to attract the destroyed hospital's patients while doing so was relatively easy. To account for the observed patterns, we would need these investments to occur disproportionately at more proximate, highly-desired hospitals.

Unfortunately, such strategic investments are difficult to observe in the data available to us. However, we can see merger activity, which might be indicative of an interest in serving affected patients. Following two disasters, we do see a hospital with a large diversion ratio from the destroyed hospital attempting to merge with the destroyed hospitals once they were rebuilt. After the Northridge earthquake, UCLA Medical Center, which had a large, underpredicted diversion, attempted to purchase St. John's, the destroyed hospital. After

merger talks broke down approximately one year following the disaster, UCLA bought Santa Monica Hospital, the only other hospital in Santa Monica. In Georgia, Sumter Regional, the destroyed hospital, merged with Phoebe Putney, which also had a large and underpredicted diversion post-disaster.

Such merger activity might reflect post-disaster strategic investments. Alternatively, rebuilding a hospital is a major capital investment and engaging in a merger may have been the best way to secure the required funds to rebuild the destroyed hospitals.

Change in Patient Composition As noted already, one possible explanation for the prediction error that we find would be changes in patient composition post-disaster. We have already restricted attention to non-elective visits, but there might have been other types of changes. For example, patients could have left the service area after the disaster, perhaps because their homes or workplaces were damaged. In Table IV, we examine this issue by reporting the number of admissions per month in the pre-disaster period compared to the post-disaster period. The number of admissions per month post-disaster falls in all service areas except NYU, ranging from 3 percent for Coney, 5 percent for St. John's, 8 percent for Bellevue, and 11 percent for Sumter and Moore. This likely reflects some extensive margin in inpatient admissions, consistent with the findings of Petek (2016) from hospital exits. We do not find major changes in case mix after the disaster, except for a rise in pregnancy admissions across the service areas (which are hard to defer) and a fall in the under 18 share of patients for Sumter and Moore. Thus, the data do not reveal obvious changes to patient populations before and after the disaster. We further examine changes in patient composition in Appendix E.

Experiment	Pre-Period	Post-Period	Percent Change
Sumter	371.20	329.20	-11.30
StJohns	2728.20	2589.20	-5.09
NYU	6335.30	6357.00	0.34
Moore	393.20	350.10	-10.95
Coney	3664.00	3560.00	-2.84
Bellevue	3650.60	3357.50	-8.03

Table IV Admissions Per Month by Period, Non-Elective Sample

Another reason why patient composition could change is that post-disaster damage could affect patients, either because they move residence, have disaster related medical complications, or face income shocks because the disaster affected their job. We examine this possibility for the Sumter, Coney, and St. John's experiments by removing zip codes with greater disaster related damage.

For Sumter, we remove the two zip codes comprising the city of Americus; the destruction of the Americus tornado was concentrated in the city of Americus. For Coney Island, we remove three zip codes which had the most amount of damage after the disaster, as based on post-disaster claims to FEMA; these zip codes are on the Long Island Sound and thus suffered more from flooding after Sandy. For St. John's, we remove zip codes with structural damage based on zip code level data from an official report on the Northridge disaster for the state of California. This procedure removes 9 zip codes, including all 5 zip codes in Santa Monica.[21]

We do not remove any areas for NYU or Bellevue, as the area immediately close to these

[21]The zip codes removed are 31719 and 31709 for Sumter; 90025, 90064, 90401, 90402, 90403, 90404, 90405, 91403, and 91436 for St. John's; and 11224, 11235, and 11229 for Coney. See http://www.arcgis.com/home/webmap/viewer.html?webmap=f27a0d274df34a77986f6e38deba2035 for Census block level estimates of Sandy damage based on FEMA reports. The US Geological Survey defines MMI values of 8 and above as causing structural damage. See ftp://ftp.ecn.purdue.edu/ayhan/Aditya/Northridge94/OES%20Reports/NR%20EQ%20Report_Part%20A.pdf, Appendix C, for the Northridge MMI data by zip code.

hospitals had very little post-Sandy damage. For Moore, removing the zip codes through which the tornado traversed would remove almost all of the patients from the choice set, so we do not conduct this robustness check for Moore.

The areas removed tend to have higher market shares for the destroyed hospital. Thus, removing destroyed areas cuts Sumter's market share from 51 percent to 30 percent, St. John's market share from 17 to 14 percent, and Coney's from 16 to 9 percent. We then compare the slope coefficient of the observed diversion ratio on the prediction error for all patients for these three experiments to just patients living in zip codes with less damage in Figure 6.3.

The magnitude of the slope coefficient is higher just examining patients that lived in locations with less disaster damage, making it unlikely that such damage can explain our results. For example, for *Semipar*, the slope coefficient is -0.37 for all patients for these three experiments, compared to -0.46 for patients living in locations with less disaster damage.

Finally, the demand models we estimate can take changes in observed patient characteristics into account when predicting diversion ratios. We do so by using estimates of all the models from pre-disaster data, as before, but estimating hospital probabilities for the post-period patients as well as pre-period patients. Formally, this estimate of the diversion ratio from j to k is the average hospital probability for k in the post-disaster period minus the average hospital probability for k in the pre-disaster period, divided by the average hospital probability for j in the pre-disaster period:

$$\hat{D}^{jk} = \frac{\frac{1}{N_{post}} \sum_{i \in I_{post}} \hat{s}_{ik} - \frac{1}{N_{pre}} \sum_{i \in I_{pre}} \hat{s}_{ik}}{\frac{1}{N_{pre}} \sum_{i \in I_{pre}} \hat{s}_{ij}}, \tag{9}$$

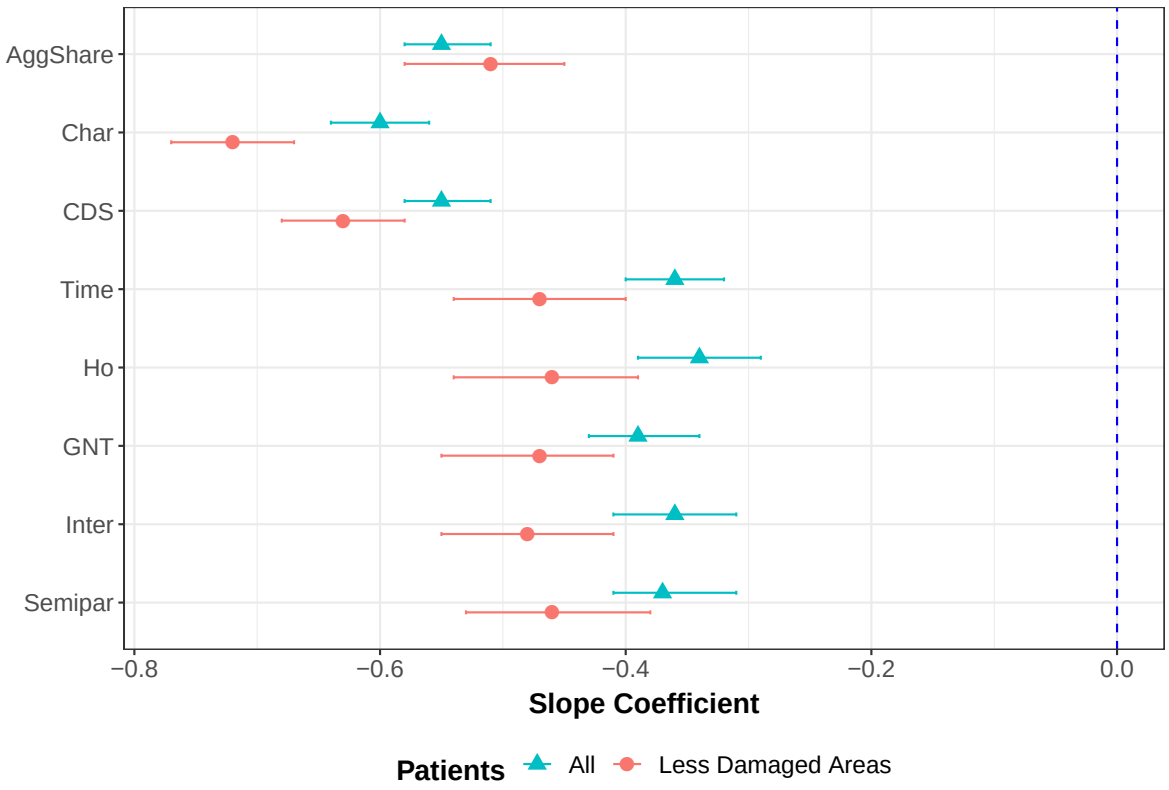

Figure 9 Slope Coefficient of Observed Diversion Ratio on Prediction Error By Disaster Damage, Non-Elective Sample

Note: The figure depicts the slope of the observed diversion ratio on the prediction error. The figure only uses data from the Coney, St. John's, or Sumter experiments, and includes either all patients or patients in zip codes with less disaster damage. Bars represent 95% confidence intervals computed from 200 bootstrap replications; we also apply a bootstrap bias correction. See Table A-7, and Table A-8 for tables of the estimates and confidence intervals used to generate this figure.

where $\hat{s}_{ik}$ is the predicted probability that patient i chooses to go to hospital k, and I_{post} and I_{pre} are the set of patients in the post-disaster period and pre-disaster period, respectively.

We find almost exactly the same patterns of underprediction of large diversion ratios using the composition adjusted estimates. For *Semipar*, the slope coefficient is -0.41 (95% CI $(-0.46,-0.36)$) after adjusting for composition, compared to -0.43 using our baseline diversion estimates.

7 Conclusion

In this paper, we compare estimates obtained from econometric models to those obtained from exogenous quasi-experiments. Our qualitative conclusions are robust across markets. First, we find that standard models of hospital demand substantially underpredict large diversion ratios. Second, models allowing spatial differentiation and including alternative specific constants are substantially better at predicting diversion ratios than other models. Third, we do not find that models that allow greater heterogeneity on observed patient characteristics, and so predict individual choices better, are also better at predicting diversion ratios.

However, even with rich micro-data, there can still be important unobserved heterogeneity in preferences. One explanation for our findings is that patients differ in their disutility for travel time, which might explain why we tend to underpredict nearby hospitals and overpredict the outside option hospital. We find a significant improvement in the prediction of diversion ratios after allowing for patient heterogeneity in travel time via random coefficients.

Separately, physician labor supply could also change due to the disaster, with physicians switching to different hospitals or not practicing during the disaster. Such changes in physician labor supply would affect patient choice when physician referral patterns are important. Better understanding how physician choice interacts with hospital choice is extremely important, especially as mergers that combine hospitals and physician groups have become more common.

Overall, the main potential limitation of our findings lies in the difference between a

hospital becoming unavailable to patients as a result of a natural disaster and a hospital becoming unavailable as a result of an inability to agree on contractual terms. First, the aftermath of the disaster may induce more short run changes in patient behavior than a network exclusion. Second, a breakdown of hospital-payer negotiations would only make the hospital unavailable to the customers of that payer, rather than all patients, and these customers could switch to a different insurer. We hope that future research can clarify the extent to which such factors could lead to different patterns than we identify here.

References

Aguirregabiria, Victor, "Empirical Industrial Organization: Models, Methods, and Applications," 2011.

Beckert, Walter and Kate Collyer, "Choice in the Presence of Experts: The Role of General Practitioners in Patients' Hospital Choice," 2017.

Berry, Steven T, "Estimating Discrete-Choice Models of Product Differentiation," *The RAND Journal of Economics*, 1994, pp. 242–262.

Capps, Cory, David Dranove, and Mark Satterthwaite, "Competition and Market Power in Option Demand Markets," *RAND Journal of Economics*, 2003, *34* (4), 737–763.

_ , Laura Kmitch, Zenon Zabinski, and Slava Zayats, "The Continuing Saga of Hospital Merger Enforcement," *Antitrust Law Journal*, 2019, *82* (2), 441–496.

Conlon, Christopher T. and Julie Holland Mortimer, "Empirical Properties of Diversion Ratios," *working paper*, 2018.

Farrell, Joseph and Carl Shapiro, "Antitrust Evaluation of Horizontal Mergers: An Economic Alternative to Market Definition," *The BE Journal of Theoretical Economics*, 2010, *10* (1), 1–39.

_ , David J. Balan, Keith Brand, and Brett W. Wendling, "Economics at the FTC: Hospital Mergers, Authorized Generic Drugs, and Consumer Credit Markets," *Review of Industrial Organization*, 2011, *39* (4), 271–296.

Garmon, Christopher, "The Accuracy of Hospital Merger Screening Methods," *The RAND Journal of Economics*, 2017, *48* (4), 1068–1102.

Gaynor, Martin, Kate Ho, and Robert J. Town, "The Industrial Organization of Health-Care Markets," *Journal of Economic Literature*, 2015, *53* (2), 235–284.

Gaynor, Martin S., Samuel A. Kleiner, and William B. Vogt, "A Structural Approach to Market Definition with an Application to the Hospital Industry," *The Journal of Industrial Economics*, 2013, *61* (2), 243–289.

Gowrisankaran, Gautam, Aviv Nevo, and Robert Town, "Mergers when Prices are Negotiated: Evidence from the Hospital Industry," *American Economic Review*, 2015, *105* (1), 172–203.

Ho, Kate and Ariel Pakes, "Hospital Choices, Hospital Prices, and Financial Incentives to Physicians," *American Economic Review*, 2014, *104* (12), 3841–3884.

_ and Robin S Lee, "Insurer competition in health care markets," *Econometrica*, 2017, *85* (2), 379–417.

_ and Robin S. Lee, "Equilibrium Provider Networks: Bargaining and Exclusion in Health Care Markets," *American Economic Review*, February 2019, *109* (2), 473–522.

Ho, Katherine, "The Welfare Effects of Restricted Hospital Choice in the US Medical Care Market," *Journal of Applied Econometrics*, 2006, *21* (7), 1039–1079.

_ , "Insurer-Provider Networks in the Medical Care Market," *The American Economic Review*, 2009, *99* (1), 393–430.

LaLonde, Robert J., "Evaluating the Econometric Evaluations of Training Programs with Experimental Data," *The American Economic Review*, 1986, pp. 604–620.

Lancaster, Kelvin J., "A New Approach to Consumer Theory," *The Journal of Political Economy*, 1966, pp. 132–157.

May, Sean M., "How Well Does Willingness-to-Pay Predict the Price Effects of Hospital Mergers?," *mimeo*, 2013.

McFadden, Daniel, Antti Talvitie, Stephen Cosslett, Ibrahim Hasan, Michael Johnson, Fred Reid, and Kenneth Train, *Demand Model Estimation and Validation*, Vol. 5, Institute of Transportation Studies, 1977.

Pathak, Parag A. and Peng Shi, "Demand Modeling, Forecasting, and Counterfactuals, Part I," Technical Report, National Bureau of Economic Research 2014.

Petek, Nathan, "The Marginal Benefit of Inpatient Hospital Treatment: Evidence from Hospital Entries and Exits," *mimeo*, 2016.

Raval, Devesh and Ted Rosenbaum, "Why Do Previous Choices Matter for Hospital Demand? Decomposing Switching Costs from Unobserved Preferences," *Review of Economics and Statistics*, 2018, *100* (5), 906–915.

_ **and** _ , "Why is Distance Important for Hospital Choice? Separating Home Bias from Transport Costs," *Journal of Industrial Economics*, forthcoming.

_ **,** _ **, and Nathan E. Wilson**, "How Do Machine Learning Algorithms Perform in Predicting Hospital Choices? Evidence from Changing Environments," *mimeo*, 2019.

_ **,** _ **, and Steven A. Tenn**, "A Semiparametric Discrete Choice Model: An Application to Hospital Mergers," *Economic Inquiry*, 2017, *55*, 1919–1944.

Shepard, Mark, "Hospital Network Competition and Adverse Selection: Evidence from the Massachusetts Health Insurance Exchange," 2016.

Todd, Petra E. and Kenneth I. Wolpin, "Assessing the Impact of a School Subsidy Program in Mexico: Using a Social Experiment to Validate a Dynamic Behavioral Model of Child Schooling and Fertility," *The American Economic Review*, 2006, pp. 1384–1417.

A Disaster Details

In this section, we give a brief narrative description of the destruction in the areas surrounding the destroyed hospitals, as well as maps for the disasters. In each figure, zip codes in the service area are outlined and disaster damage is shaded as indicated.

A.1 St. John's (Northridge Earthquake)

On January 17th, 1994, an earthquake rated 6.7 on the Richter scale hit the Los Angeles Metropolitan area 32 km northwest of Los Angeles. This earthquake killed 61 people, injured 9,000, and seriously damaged 30,000 homes. According to the USGS, the neighborhoods worst affected by the earthquake were the San Fernando Valley, Northridge and Sherman Oaks, while the neighborhoods of Fillmore, Glendale, Santa Clarita, Santa Monica, Simi Valley and western and central Los Angeles also suffered significant damage.[22] Over 1,600 housing units in Santa Monica alone were damaged with a total cost of $70 million.[23]

Figure 14 shows that the damage in the Los Angeles area was more widespread than the other disasters; we depict the intensity of earthquake shaking with darker green shading. While the Santa Monica area was particularly hard hit, many areas nearby received little structural damage from the earthquake.

The earthquake damaged a number of major highways of the area; in our service area, the most important was the I-10 (Santa Monica Freeway) that passed through Santa Monica. It reopened on April 11, 1994.[24] By the same time, many of those with damaged houses had found new housing.[25]

Santa Monica Hospital, located close to St. John's, remained open but at a reduced capacity of 178 beds compared to 298 beds before the disaster. In July 1995, Santa Monica Hospital merged with UCLA Medical Center.[26] St. John's hospital reopened for inpatient services on October 3, 1994, although with only about half of the employees and inpatient beds and without its North Wing (which was razed).[27]

A.2 Sumter (Americus Tornado)

On March 1, 2007, a tornado went through the center of the town of Americus, GA, damaging 993 houses and 217 businesses. The tornado also completely destroyed Sumter Regional Hospital. An inspection of the damage map in Figure 1 and GIS maps of destroyed structures suggests that the damage was relatively localized – the northwest part of the city was not damaged, and very few people in the service area outside of the town of Americus were affected.[28] Despite the tornado, employment remains roughly constant in the Americus Micropolitan Statistical Area after the disaster, at 15,628 in February 2007 before the disaster and 15,551 in February 2008 one year

[22] See http://earthquake.usgs.gov/earthquakes/states/events/1994_01_17.php.

[23] See http://smdp.com/santa-monicans-remember-northridge-earthquake/131256.

[24] See http://articles.latimes.com/1994-04-06/news/mn-42778_1_santa-monica-freeway.

[25] See http://www.nytimes.com/1994/03/17/us/los-angeles-is-taking-rapid-road-to-recovery.html?pagewanted=all.

[26] See http://articles.latimes.com/1995-07-21/business/fi-26439_1_santa-monica-hospital-medical-center.

[27] See http://articles.latimes.com/1994-09-23/local/me-42084_1_inpatient-services.

[28] See https://www.georgiaspatial.org/gasdi/spotlights/americus-tornado for the GIS map.

later.[29]

While Sumter Regional slowly re-introduced some services such as urgent care, they did not reopen for inpatient admissions until April 1, 2008 in a temporary facility with 76 beds and 71,000 sq ft of space. Sumter Regional subsequently merged with Phoebe Putney Hospital in October 2008, with the full merge completed on July 1, 2009. On December 2011, a new facility was built with 76 beds and 183,000 square feet of space.[30]

A.3 NYU, Bellevue, and Coney Island (Superstorm Sandy)

Superstorm Sandy hit the New York Metropolitan area on October 28th - 29th, 2012. The storm caused severe localized damage and flooding, shutdown the New York City Subway system, and caused many people in the area to lose electrical power. By November 5th, normal service had been restored on the subways (with minor exceptions).[31] Major bridges reopened on October 30th and NYC schools reopened on November 5th.[32] By November 5th, power was restored to 70 percent of New Yorkers, and to all New Yorkers by November 15th.

FEMA damage inspection data reveals that most of the damage from Sandy occured in areas adjacent to water.[33]

We depict the flooding from Hurricane Sandy in Figure 11 to Figure 13 for each of the service areas in green shading. Flooding primarily affected areas adjacent to water. The actual damage in Manhattan from Sandy – most of which classified by FEMA as "Minor" damage – was concentrated in a relatively small part of the Manhattan hospitals' service areas. For Coney Island, most of the flooding affected the three zip codes at the bottom of the service area that are directly adjacent to Long Island Sound. Even at the island tip, most block groups suffered less than 50 percent damage.

NYU Langone Medical Center suffered about $1 billion in damage due to Sandy, with its main generators flooded. While some outpatient services reopened in early November, it only partially reopened inpatient services on December 27, 2012, including some surgical services and medical and surgical intensive care. The maternity unit and pediatrics reopened on January 14th, 2013. [34] While NYU Langone opened an urgent care center on January 17, 2013, a true emergency room did not open until April 24, 2014, more than a year later.[35]

Bellevue Hospital Center reopened limited outpatient services on November 19th, 2012.[36] However, Bellevue did not fully reopen inpatient services until February 7th, 2013.[37] Coney Island Hospital opened an urgent care center by December 3, 2012, but patients were not admitted inpatient.

[29] See http://beta.bls.gov/dataViewer/view/timeseries/LAUMC131114000000005;jsessionid=212BF9673EB816FE50F37957842D1695.tc_instance6.

[30] See https://www.phoebehealth.com/phoebe-sumter-medical-center/phoebe-sumter-medical-center-about-us and http://www.wtvm.com/story/8091056/full-medical-services-return-to-americus-after-opening-of-sumter-regional-east.

[31] See http://web.mta.info/sandy/timeline.htm.

[32] See http://www.cnn.com/2013/07/13/world/americas/hurricane-sandy-fast-facts/.

[33] See the damage map at https://www.huduser.gov/maps/map_sandy_blockgroup.html.

[34] See http://www.cbsnews.com/news/nyu-langone-medical-center-partially-reopens-after-sandy/.

[35] See http://fox6now.com/2013/01/17/nyu-medical-center-reopens-following-superstorm-sandy/ and http://www.nytimes.com/2014/04/25/nyregion/nyu-langone-reopens-emergency-room-that-was-closed-by-hurricane-sandy.html.

[36] See http://www.cbsnews.com/news/bellevue-hospital-in-nyc-partially-reopens/.

[37] See http://www.nbcnewyork.com/news/local/Bellevue-Hospital-Reopens-Sandy-Storm-East-River-Closure-190298001.html.

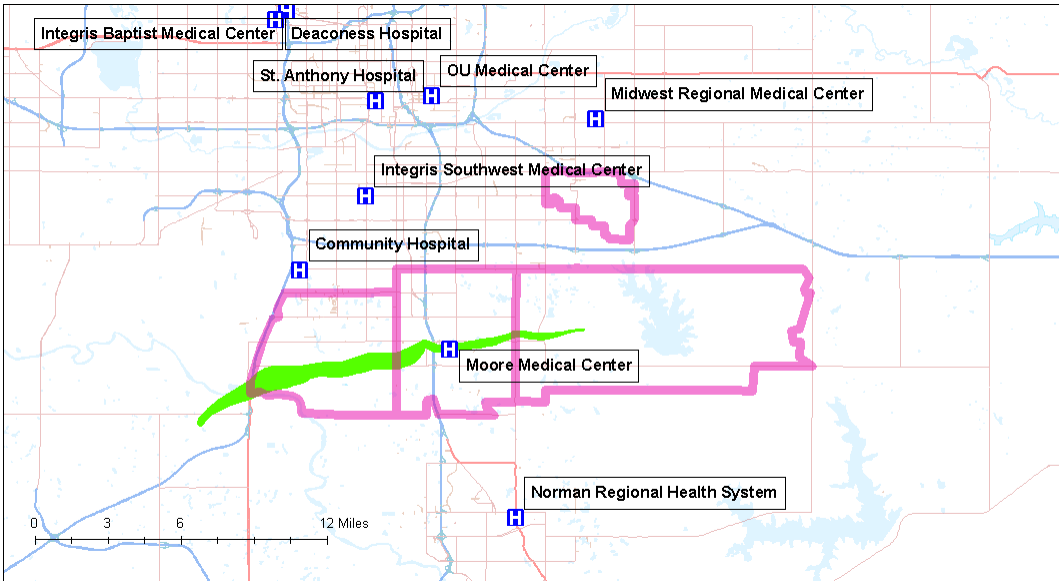

Figure 10 Damage Map in Moore, OK

Note: The green area indicates the damage path of the tornado. The zip codes included in the service area are outlined in pink. Sources: NOAA, OK Discharge Data

It had reopened ambulance service and most of its inpatient beds by February 20th, 2013, although at that time trauma care and labor and delivery remained closed. The labor and delivery unit did not reopen until June 13th, 2013.[38]

A.4 Moore (Moore Tornado)

A tornado went through the Oklahoma City suburb of Moore on May 20, 2013. The tornado destroyed two schools and more than 1,000 buildings (damaging more than 1,200 more) in the area of Moore and killed 24 people. Interstate 35 was briefly closed for a few hours due to the storm.[39] We depict the tornado's path in Figure 10 in green; while some areas were severely damaged, nearby areas were relatively unaffected.[40]

Emergency services, but not inpatient admissions, temporarily reopened at Moore Medical Center on December 2, 2013. Groundbreaking for a new hospital took place on May 20, 2014, and the new hospital reopened in May 2016.[41]

[38] See http://www.sheepsheadbites.com/2012/12/coney-island-hospital-reopens-urgent-care-center/, http://www.sheepsheadbites.com/2013/02/coney-island-hospital-reopens-er-limited-911-intake/, and http://www.sheepsheadbites.com/2013/06/photo-first-post-sandy-babies-delivered-at-coney-island-hospital-after-labor-and-delivery-unit-reopens/.

[39] See http://www.news9.com/story/22301266/massive-tornado-kills-at-least-51-in-moore-hits-elementary-school.

[40] See http://www.srh.noaa.gov/oun/?n=events-20130520 and http://www.nytimes.com/interactive/2013/05/20/us/oklahoma-tornado-map.html for maps of the tornado's path.

[41] See https://www.normanregional.com/en/locations.html?location_list=2 and http://kfor.com/2013/11/20/moore-medical-center-destroyed-in-tornado-to-reopen-in-december/.

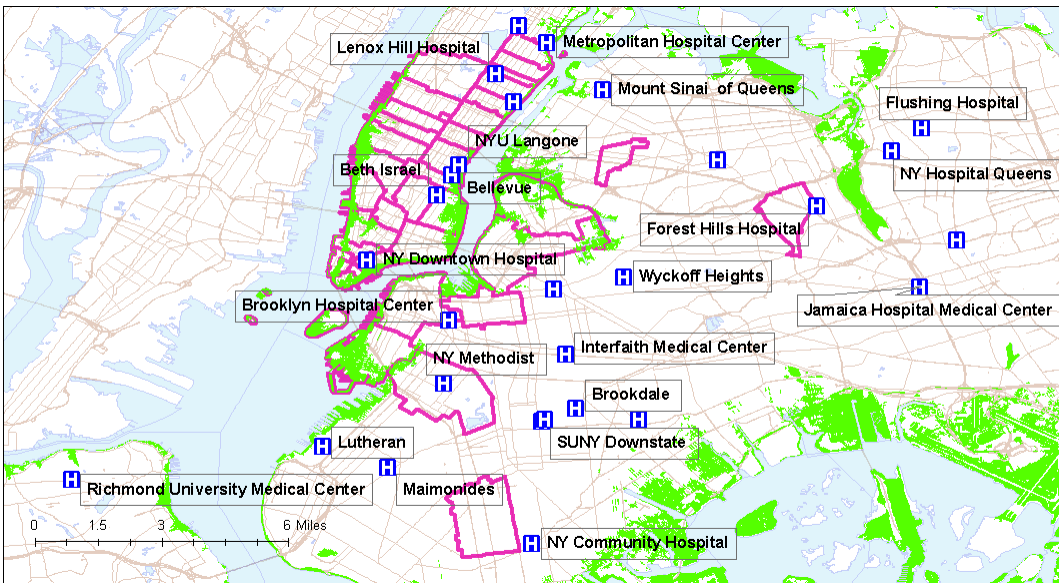

Figure 11 Damage Map for NYU Service Area

Note: Green shading represents flooded areas. The zip codes included in the service area are outlined in pink. Sources: FEMA, NY Discharge Data

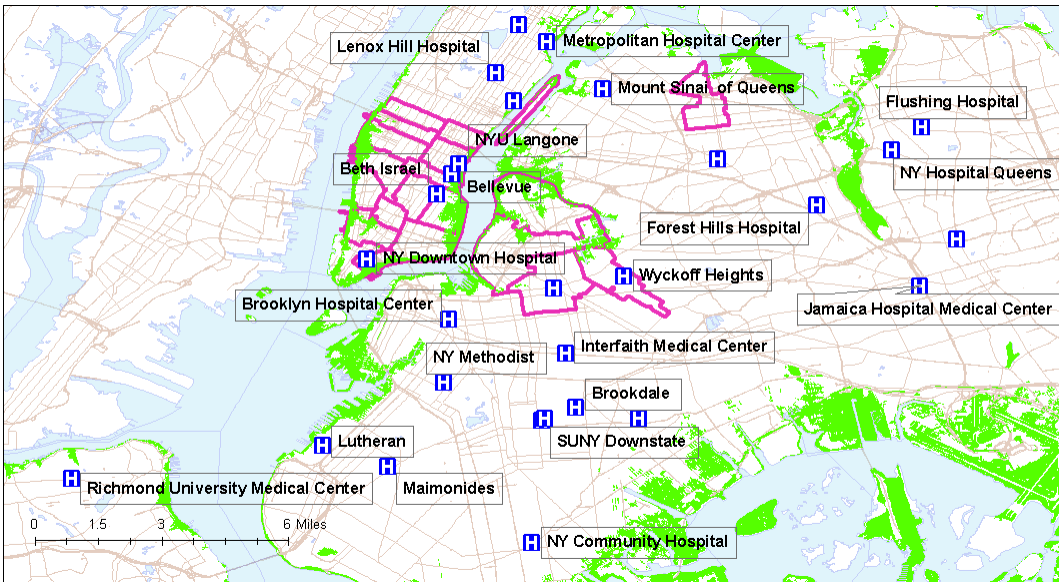

Figure 12 Damage Map for Bellevue Service Area

Note: Green shading represents flooded areas. The zip codes included in the service area are outlined in pink. Sources: FEMA, NY Discharge Data

B Dataset Construction

This section provides more detail on the information in Table I. For each disaster, we estimate models on the pre-period prior to the disaster and then validate them on the period after the disaster. We omit the month of the disaster from either period, excluding anyone either admitted

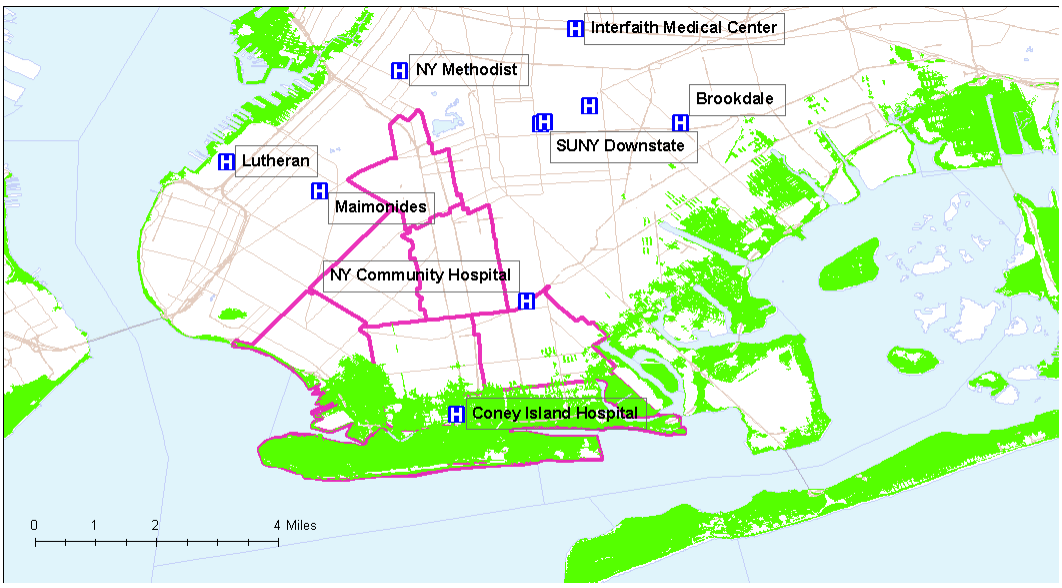

Figure 13 Damage Map for Coney Island Service Area

Note: Green shading represents flooded areas. The zip codes included in the service area are outlined in pink. Sources: FEMA, NY Discharge Data

or discharged in the disaster month. The length of the pre-period and post-period in general depends upon the length of the discharge data that we have available. Table Ib contains the disaster date and the pre-period and post-period for each disaster, where months are defined by time of admission.

NYU hospital began limited inpatient service on December 27, 2012; unfortunately, we only have month and not date of admission and so cannot remove all patients admitted after December 27th. Right now, we drop 65 patients admitted in December to NYU; this patient population is very small compared to the size and typical capacity of NYU.

For California, we exclude all patients going to Kaiser hospitals, as Kaiser is a vertically integrated insurer and almost all patients with Kaiser insurance go to Kaiser hospitals, and very few patients without Kaiser insurance go to Kaiser hospitals. This is in line with the literature examining hospital choice in California including Capps et al. (2003). We also exclude February though April 1994, as the I-10 Santa Monica freeway that goes through Santa Monica only reopens in April.

C Details on the *Semipar* Estimator

This section provides details on the *Semipar* estimator described in the text. This estimator is nearly identical to that described in Raval et al. (2017).

In contrast to the other estimation approaches in the text, *Semipar* models hospitals in product space. In particular, this approach estimates alternative specific constants for each group of patients (indexed by g).

$$s_j^g = \frac{e^{\delta_j^g}}{\sum_{k \in J} e^{\delta_k^g}}.$$

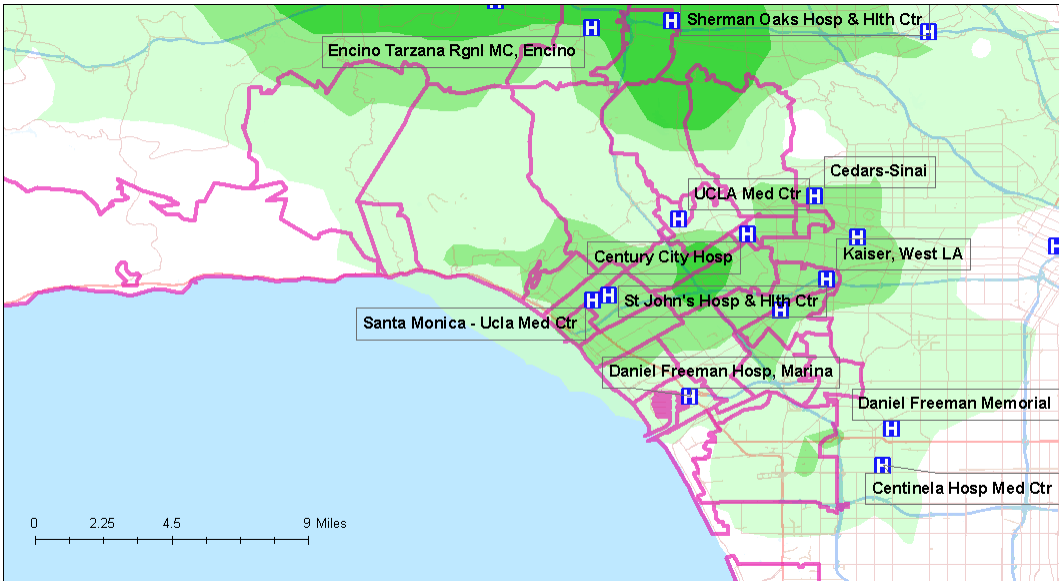

Figure 14 Damage Map in Los Angeles, CA

Note: Darker green areas indicate the earthquake intensity measured by the Modified Mercalli Intensity (MMI); an MMI value of 7 reflects non-structural damage and a value of 8 moderate structural damage. The areas that experienced the quake with greater intensity were shaded in a darker color, with the MMI in the area ranging from 7-8.6. Any areas with an MMI of below 7 were not colored. The zip codes included in the service area are outlined in pink. Sources: USGS Shakemap, OSHPD Discharge Data

Given group assignments and data on shares for each hospital j recovering $e^{\delta_j^g}$ is straightforward to compute from the equation above by using the inversion from Berry (1994).

Therefore, the key choices for the researcher in this model involve how to assign patients to groups. In our application, all patients are assigned a group based upon their zip code, disease acuity (DRG weight), age group, and area of diagnosis (MDC). Anyone in a group above the minimum group size is assigned choice probabilities based upon the share of patients in that group that go to each hospital. Then, we drop a characteristic, reconstruct groups, and again compute group-level shares for the full set of patients, both those previously grouped and those not previously grouped.[42] All patients who have not yet been assigned a choice probability and are in groups above the minimum group size are assigned a choice probability based on that round's group-level shares. We continue until there are no more covariates to group or until all patients are assigned a choice probability.[43] We drop characteristics in the reverse order listed above (i.e., MDC, age group, etc.).

The minimum group size regulates the bias-variance tradeoff; increasing the minimum group size increases the bias but reduces variance. For this paper, we use a minimum group size of 50. Our approach is equivalent to estimating different multinomial logit models with group-specific alternative specific constants for each level of grouping and assigning choice probabilities to an individual based upon the most refined level of grouping that exceeds the pre-specified minimum

[42] Raval et al. (2017) used previously non-grouped individuals to compute the choice probabilities. The approach in this paper will have a higher bias, but relatively smaller variance. The approach in this paper is analogous to the one in Raval et al. (2019).

[43] In this last round of grouping, we do not impose a minimum group size restriction. So, for example, if a zip code only has 10 residents, we compute choice probabilities based upon these 10 people.

group size. Once the researcher has constructed the set of groups, predicted choice probabilities can be estimated as the empirical shares of hospitals within each group.

Since in this approach one estimates many fixed effects in a non-linear model, there are a number of potential concerns. First, one may be concerned that due to an incidental parameters problem, our main parameter estimates will not be consistently estimated. However, in this approach, the researcher directly estimates the group level choice probabilities, which are the main parameters of interest. Therefore, there are no incidental parameters being estimated. Second, one may worry that the estimates of the group level choice probabilities are not consistent or are estimated with significant variance in finite samples. However, the combination of an imposed minimum group size and a finite number of possible groups means that the estimates should converge for sufficiently large group sizes. In this paper, we are able to test the finite sample performance of this estimator, and should observe the model's performance suffer to the extent that these parameters are imprecisely estimated.

Finally, since the group sizes are relatively small, there is a potential concern that an individual's observed choice has an important effect on their predicted choice. To address this concern, in computing individual i's mean utility for hospital j ($\hat{\delta}_k^{i(g)}$), we leave out individual i by computing s_j^g excluding individual i.

D Estimation Details

In Table V to Table XVI below, we report estimation details for all of the models except *Semipar*, including the number of parameters in the model, the estimated log likelihood of the model, the AIC and BIC criteria, and McFadden's pseudo R^2. We provide these details for both the non-elective sample and the full sample.

The total number of observations for each experiment is the number of admissions in the pre-period multiplied by the number of choices. Thus, the total number of observations for the non-elective sample was 75,492 for Moore, 1,083,342 for NYU, 560,592 for Coney, 657,100 for Bellevue, 77,955 for Sumter, and 1,432,305 for St John's. The total number of observations for the full sample was 117,156 for Moore, 1,519,050 for NYU, 791,996 for Coney, 916,263 for Bellevue, 104,100 for Sumter, and 2,030,091 for St John's.

Table V Estimation Details for Moore, Non-Elective Sample

Model	No. Parameters	Log Likelihood	AIC	BIC	Pseudo R^2
AggShare	11.00	-14480.24	28982.49	29084.04	0.07
Char	20.00	-14253.20	28546.40	28731.04	0.09
CDS	51.00	-13631.99	27365.97	27836.79	0.13
Time	13.00	-14273.72	28573.44	28693.45	0.09
Ho	51.00	-13991.55	28085.10	28555.92	0.10
GNT	36.00	-13858.01	27788.02	28120.37	0.11
Inter	122.00	-12974.07	26190.14	27307.18	0.17

Note: All models estimated on the non-elective sample. The second column is the number of parameters in the model, the third column the estimated log likelihood of the model, the fourth and fifth columns the AIC and BIC criteria, and the sixth column McFadden's pseudo R^2.

Table VI Estimation Details for NYU, Non-Elective Sample

Model	No. Parameters	Log Likelihood	AIC	BIC	Pseudo R^2
AggShare	18	-148420.61	296877.23	297091.35	0.12
Char	20	-118967.96	237969.93	238172.15	0.29
CDS	51	-115203.01	230506.02	231100.80	0.31
Time	20	-113485.05	227010.10	227248.02	0.32
Ho	58	-110106.66	220315.33	220922.00	0.34
GNT	50	-111472.56	223043.12	223626.00	0.34
Inter	185	-107852.65	216073.31	218262.09	0.36

Note: All models estimated on the non-elective sample. The second column is the number of parameters in the model, the third column the estimated log likelihood of the model, the fourth and fifth columns the AIC and BIC criteria, and the sixth column McFadden's pseudo R^2.

Table VII Estimation Details for Coney, Non-Elective Sample

Model	No. Parameters	Log Likelihood	AIC	BIC	Pseudo R^2
AggShare	16	-75843.46	151718.93	151898.72	0.19
Char	20	-80677.82	161389.64	161580.67	0.14
CDS	51	-72383.05	144868.10	145441.18	0.23
Time	18	-73253.35	146542.70	146744.96	0.22
Ho	56	-70937.26	141972.52	142523.12	0.24
GNT	46	-72750.39	145590.78	146096.44	0.22
Inter	167	-70237.82	140807.64	142672.94	0.25

Note: All models estimated on the non-elective sample. The second column is the number of parameters in the model, the third column the estimated log likelihood of the model, the fourth and fifth columns the AIC and BIC criteria, and the sixth column McFadden's pseudo R^2.

E Case Mix

In this section, we examine how the case mix changed from the period before the disaster to the period after the disaster. In Table XVII, we examine changes in case mix across a set of variables including age, fraction aged less than 18, fraction aged above 64, diagnosis acuity (DRG weight), fraction emergency, fraction circulatory diagnosis (MDC 5), fraction labor/pregnancy diagnosis (MDC 14), fraction using a commercial payer, fraction using Medicare, and average number of admissions per month. We report the percent change for the variable in the post-period compared to pre-period. Table XVII is based upon the full sample, while Table XVIII is based upon the non-elective sample. We summarize results for the full sample below.

There are no large changes in age across the hospitals, except that the fraction admitted under 18 falls by 23 percent for Moore and 45 percent for Sumter. Diagnosis acuity does not change much after the disasters. The only large change in type of insurance is for Sumter, where the fraction of commercial insurance falls by about 30 percent after the disaster. We examined this change; the fraction of patients reporting "Unspecified Other" payer rises precipitously in the first quarter after the disaster, and then falls back to a small fraction of patients. Our belief is that this reflects improper coding post-disaster.

Table VIII Estimation Details for Bellevue, Non-Elective Sample

Model	No. Parameters	Log Likelihood	AIC	BIC	Pseudo R^2
AggShare	19	-82180.46	164398.92	164615.24	0.16
Char	20	-74312.75	148657.51	148839.68	0.24
CDS	51	-72050.89	144201.77	144771.06	0.27
Time	21	-70584.41	141210.82	141449.92	0.28
Ho	59	-67881.36	135866.72	136458.78	0.31
GNT	52	-69888.13	139878.26	140458.93	0.29
Inter	194	-67811.66	136009.32	138206.75	0.31

Note: All models estimated on the non-elective sample. The second column is the number of parameters in the model, the third column the estimated log likelihood of the model, the fourth and fifth columns the AIC and BIC criteria, and the sixth column McFadden's pseudo R^2.

Table IX Estimation Details for Sumter, Non-Elective Sample

Model	No. Parameters	Log Likelihood	AIC	BIC	Pseudo R^2
AggShare	14	-8343.83	16715.66	16845.36	0.41
Char	20	-6480.57	13001.14	13186.42	0.54
CDS	51	-6186.46	12472.91	12936.11	0.56
Time	16	-6261.38	12554.76	12702.98	0.56
Ho	54	-5875.31	11858.61	12358.86	0.58
GNT	42	-5924.61	11931.21	12311.03	0.58
Inter	149	-5370.74	11037.47	12408.53	0.62

Note: All models estimated on the non-elective sample. The second column is the number of parameters in the model, the third column the estimated log likelihood of the model, the fourth and fifth columns the AIC and BIC criteria, and the sixth column McFadden's pseudo R^2.

The fraction of labor/pregnancy diagnosis rises in all service areas, and by more than 10 percent for Bellevue and Coney, which may be because pregnancies cannot be postponed or ignored and so have no extensive margin. Overall, we do not find major changes in case mix after the disaster, except for the rise in pregnancy admissions across the service areas and the fall in the under 18 share for Sumter and Moore.

Table X Estimation Details for St John's, Non-Elective Sample

Model	No. Parameters	Log Likelihood	AIC	BIC	Pseudo R^2
AggShare	20	-168172.34	336384.67	336628.10	0.19
Char	20	-155353.88	310747.76	310991.18	0.25
CDS	51	-146277.59	292657.17	293277.90	0.29
Time	22	-144297.12	288638.24	288906.01	0.30
Ho	60	-141634.94	283389.88	284120.15	0.32
GNT	54	-141488.72	283085.44	283742.68	0.32
Inter	203	-136753.56	273911.12	276369.69	0.34

Note: All models estimated on the non-elective sample. The second column is the number of parameters in the model, the third column the estimated log likelihood of the model, the fourth and fifth columns the AIC and BIC criteria, and the sixth column McFadden's pseudo R^2.

Table XI Estimation Details for Moore, Full Sample

Model	No. Parameters	Log Likelihood	AIC	BIC	Pseudo R^2
AggShare	11	-22331.56	44685.12	44791.51	0.08
Char	20	-22083.47	44206.95	44400.37	0.09
CDS	51	-21075.79	42253.58	42746.81	0.13
Time	13	-21982.78	43991.56	44117.29	0.09
Ho	51	-21548.72	43199.43	43692.67	0.11
GNT	36	-21405.45	42882.90	43231.06	0.12
Inter	122	-20084.84	40411.67	41581.90	0.17

Note: All models estimated on the full sample. The second column is the number of parameters in the model, the third column the estimated log likelihood of the model, the fourth and fifth columns the AIC and BIC criteria, and the sixth column McFadden's pseudo R^2.

Table XII Estimation Details for NYU, Full Sample

Model	No. Parameters	Log Likelihood	AIC	BIC	Pseudo R^2
AggShare	18	-211848.84	423733.68	423953.88	0.10
Char	20	-171159.33	342352.66	342560.63	0.27
CDS	51	-163021.86	326143.72	326755.40	0.31
Time	20	-164552.98	329145.95	329390.62	0.30
Ho	58	-159893.26	319888.53	320512.44	0.32
GNT	50	-162076.84	324251.68	324851.12	0.31
Inter	185	-158610.38	317588.75	319839.73	0.33

Note: All models estimated on the full sample. The second column is the number of parameters in the model, the third column the estimated log likelihood of the model, the fourth and fifth columns the AIC and BIC criteria, and the sixth column McFadden's pseudo R^2.

Table XIII Estimation Details for Coney, Full Sample

Model	No. Parameters	Log Likelihood	AIC	BIC	Pseudo R^2
AggShare	16	-109623.34	219278.68	219464	0.17
Char	20	-114909.94	229853.89	230050.78	0.13
CDS	51	-103857.15	207814.29	208393.41	0.21
Time	18	-105906.74	211849.48	212057.96	0.20
Ho	56	-102327.91	204753.82	205321.35	0.22
GNT	46	-105114.44	210318.87	210840.08	0.20
Inter	167	-101809.59	203951.17	205873.83	0.23

Note: All models estimated on the full sample. The second column is the number of parameters in the model, the third column the estimated log likelihood of the model, the fourth and fifth columns the AIC and BIC criteria, and the sixth column McFadden's pseudo R^2.

Table XIV Estimation Details for Bellevue, Full Sample

Model	No. Parameters	Log Likelihood	AIC	BIC	Pseudo R^2
AggShare	19	-117919.64	235877.28	236100.11	0.15
Char	20	-104182.25	208396.50	208584.14	0.25
CDS	51	-101134.46	202368.91	202955.32	0.27
Time	21	-100109.69	200261.38	200507.66	0.28
Ho	59	-96684.78	193473.55	194083.41	0.30
GNT	52	-99120.44	198342.88	198941.01	0.28
Inter	194	-96544.97	193475.94	195739.46	0.30

Note: All models estimated on the full sample. The second column is the number of parameters in the model, the third column the estimated log likelihood of the model, the fourth and fifth columns the AIC and BIC criteria, and the sixth column McFadden's pseudo R^2.

Table XV Estimation Details for Sumter, Full Sample

Model	No. Parameters	Log Likelihood	AIC	BIC	Pseudo R^2
AggShare	14	-11914.76	23857.52	23991.27	0.37
Char	20	-9676.37	19392.74	19583.81	0.49
CDS	51	-9029.20	18158.40	18636.06	0.52
Time	16	-9386.21	18804.43	18957.28	0.50
Ho	49	-8876.75	17851.50	18319.61	0.53
GNT	42	-8699.91	17481.82	17873.50	0.54
Inter	149	-8094.26	16484.51	17898.37	0.57

Note: All models estimated on the full sample. The second column is the number of parameters in the model, the third column the estimated log likelihood of the model, the fourth and fifth columns the AIC and BIC criteria, and the sixth column McFadden's pseudo R^2.

Table XVI Estimation Details for St John's, Full Sample

Model	No. Parameters	Log Likelihood	AIC	BIC	Pseudo R^2
AggShare	20	-239495.27	479030.54	479281.01	0.19
Char	20	-225640.76	451321.52	451571.99	0.24
CDS	51	-215470.24	431042.48	431681.18	0.27
Time	22	-209454.45	418952.89	419228.41	0.29
Ho	60	-206835.28	413790.55	414541.97	0.30
GNT	54	-206498.56	413105.13	413781.40	0.30
Inter	203	-199907.05	400218.11	402747.87	0.32

Note: All models estimated on the full sample. The second column is the number of parameters in the model, the third column the estimated log likelihood of the model, the fourth and fifth columns the AIC and BIC criteria, and the sixth column McFadden's pseudo R^2.

Table XVII Post-Disaster Changes in Case-Mix, in Percent Change from Pre-Period, Full Sample

Variable	Sumter	Moore	NYU	Bellevue	Coney	StJohns
Age	1.09	0.12	0.94	2.36	0.11	-0.98
	(-0.6,2.52)	(-1.39,1.56)	(0.35,1.63)	(1.28,3.28)	(-0.82,1.15)	(-1.67,-0.31)
Age < 18	-45.43	-23.73	2.84	-12.54	2.41	11.72
	(-55.59,-37.22)	(-34.92,-12.86)	(-4.22,10.39)	(-22.07,-4.16)	(-7.43,11.06)	(3.39,19.34)
Age > 64	-4.28	-2.88	4.74	9.01	3	-2.07
	(-8.79,0.23)	(-6.93,1.33)	(3.11,6.34)	(5.76,11.86)	(0.68,5.5)	(-3.84,-0.17)
Diagnosis Acuity	3.72	2.12	1.02	3.29	3.29	3.3
	(0.29,7.02)	(-1.35,5.53)	(-0.51,2.61)	(0.67,6.14)	(1.12,6.07)	(1.68,5.1)
Emergency	-11.34	18.02	2.47	0.44	-7.51	-1.22
	(-15.88,-7.3)	(11.29,24.57)	(1.04,3.74)	(-1.04,1.88)	(-8.88,-6.01)	(-3.46,0.7)
Circulatory Diagnosis	11.28	-12.1	-7.82	-7.04	-5.24	5.49
	(3.68,19.63)	(-22.4,-2.78)	(-11.57,-4.5)	(-12.47,-1.95)	(-9.15,-0.87)	(1.61,9.28)
Labor/Pregnancy Diagnosis	7.36	7.05	7.03	10.51	13.62	5.62
	(-2.03,15.61)	(0.38,13.78)	(3.89,10.24)	(5.16,15.25)	(7.78,19.11)	(2.43,9.22)
Commercial Payer	-28.41	3.88	-2.84	-2.06	-6.08	6.19
	(-33.45,-24.22)	(-1.13,7.92)	(-5.07,-0.27)	(-5.73,1.55)	(-10.12,-2.13)	(4.52,8.02)
Medicare Payer	-4.94	-1.91	4.91	9.24	2.18	-8.79
	(-8.32,-1.35)	(-5.19,2.24)	(3.07,6.75)	(6.19,11.98)	(-0.05,4.49)	(-10.8,-6.58)

Note: Estimates based upon the Full Sample. Each cell reports the percent change for a given variable in the post-period compared to pre-period for a given experiment, along with the 95% confidence interval.

Table XVIII Post-Disaster Changes in Case-Mix, in Percent Change from Pre-Period, Non-Elective Sample

Variable	Sumter	Moore	NYU	Bellevue	Coney	StJohns
Age	0.28	-1.66	1.34	1.49	-0.07	-1.99
	(-1.45,2.42)	(-3.72,0.07)	(0.64,2.03)	(0.22,2.71)	(-1.16,0.93)	(-2.9,-1.13)
Age < 18	-33.26	-21.66	8.38	-8.94	4.06	10.91
	(-45.07,-21.49)	(-38.38,-5.75)	(-2.45,18.26)	(-18.9,1.28)	(-6.87,15.45)	(2.44,20.17)
Age > 64	-4.79	-5.74	6.37	7.29	2.5	-5.31
	(-10.4,-0.29)	(-12.58,-0.23)	(4.39,8.77)	(2.79,11.21)	(-0.17,5.35)	(-7.65,-3.33)
Diagnosis Acuity	4.68	-1.29	2.84	3.08	4.03	2.69
	(1.07,8.64)	(-4.92,2.3)	(0.88,4.87)	(0.13,6.14)	(1.28,6.67)	(0.22,5.01)
Emergency	-14.68	18.38	2.06	0.45	-8.5	-2.2
	(-18,-11.08)	(8.53,26.89)	(0.76,3.39)	(-1.71,2.37)	(-10.25,-7.08)	(-3.88,-0.5)
Circulatory Diagnosis	6.15	-7.54	-7.96	-8.53	-7.41	1.42
	(-3.9,15.08)	(-26.05,11.01)	(-12.34,-3.67)	(-14.62,-3.57)	(-13,-2.1)	(-2.02,5.09)
Labor/Pregnancy Diagnosis	3.76	11.86	2.94	10.81	9.77	4.55
	(-6.05,12)	(3.13,18.19)	(-0.27,5.93)	(5.79,17.17)	(4.67,15.12)	(1.19,8.11)
Commercial Payer	-27.46	3.89	1.33	-0.72	-7.33	6.19
	(-33.2,-22.56)	(-2.77,9.57)	(-1.28,3.95)	(-5.13,3.24)	(-12.05,-1.8)	(3.85,8.28)
Medicare Payer	-8.4	-6.2	5.33	7.25	1.77	-11.48
	(-12.83,-3.53)	(-11.64,-1.35)	(3.13,7.39)	(3.55,10.73)	(-0.72,4.41)	(-13.72,-9.47)

Note: Estimates based upon the non-elective sample. Each cell reports the percent change for a given variable in the post-period compared to pre-period for a given experiment, along with the 95% confidence interval.

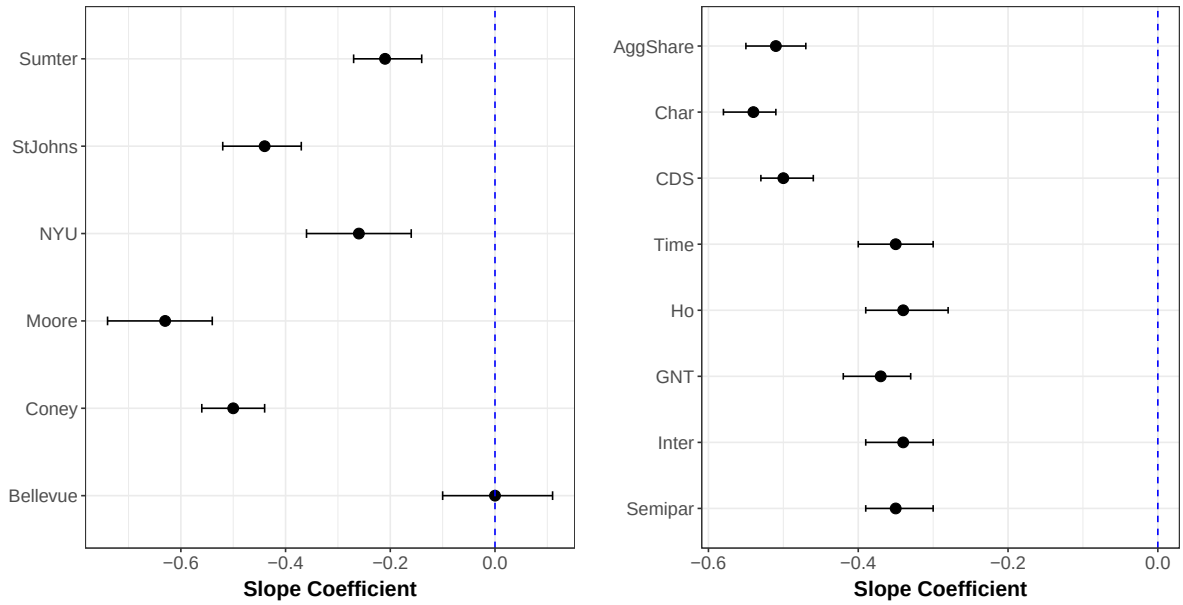

(a) By Experiment (for *Semipar*) (b) By Model

Figure A-1 Slope Coefficient of Observed Choice Removal Diversion Ratios on Prediction Error, Non-Elective Sample

Note: The left figure depicts the slope of the observed diversion ratio on the prediction error by model, while the right figure depicts the same by experiment for the *Semipar* model. Bars represent 95% confidence intervals computed from 200 bootstrap replications; we also apply a bootstrap bias correction. See Table A-10 and Table A-11 for tables of the estimates and confidence intervals used to generate these figures.

For Online Publication

F Supplemental Figures: Full Sample

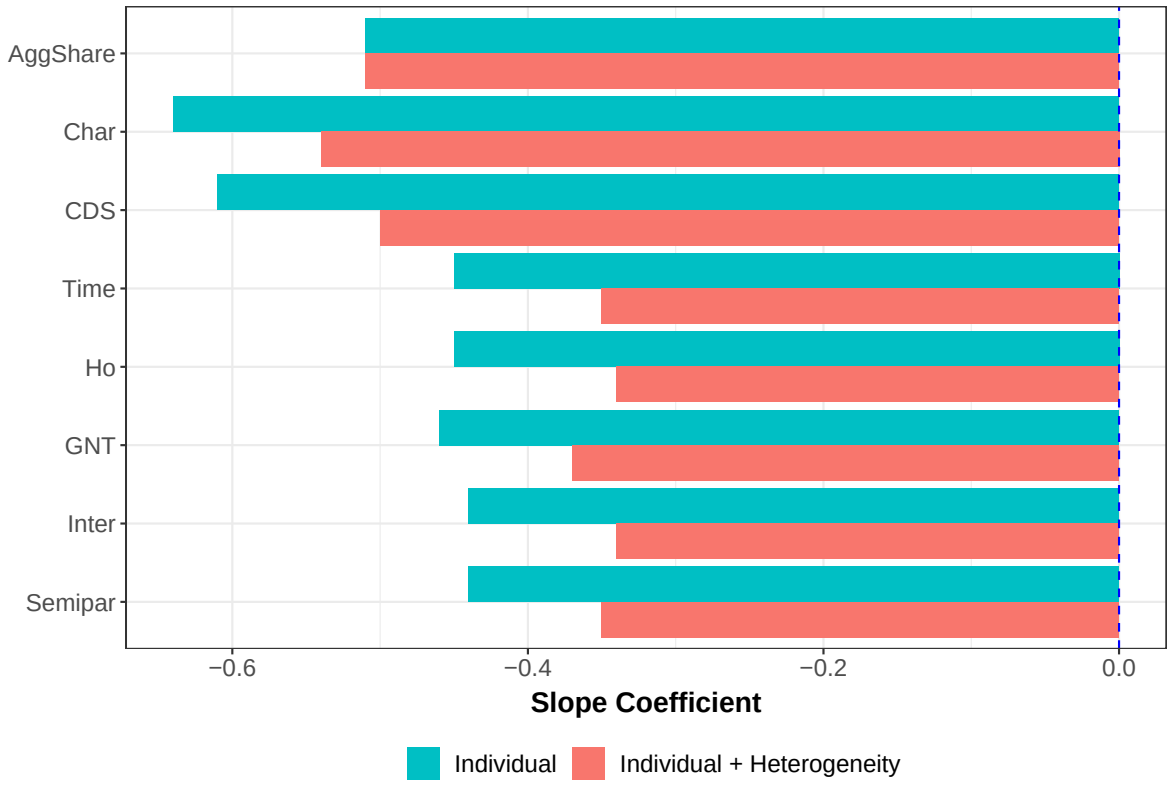

Figure A-2 Decomposition of Average Predicted Diversion, Full Sample

Note: We report the slope coefficient of the observed diversion ratio on the prediction error based upon the average individual diversion ratio in blue, and based upon the individual diversion ratio plus the heterogeneity factor (i.e. the total predicted diversion) in red, for each model. Each term is as defined in the text. See Table A-12 for a table of the estimates and confidence intervals used to generate this figure.

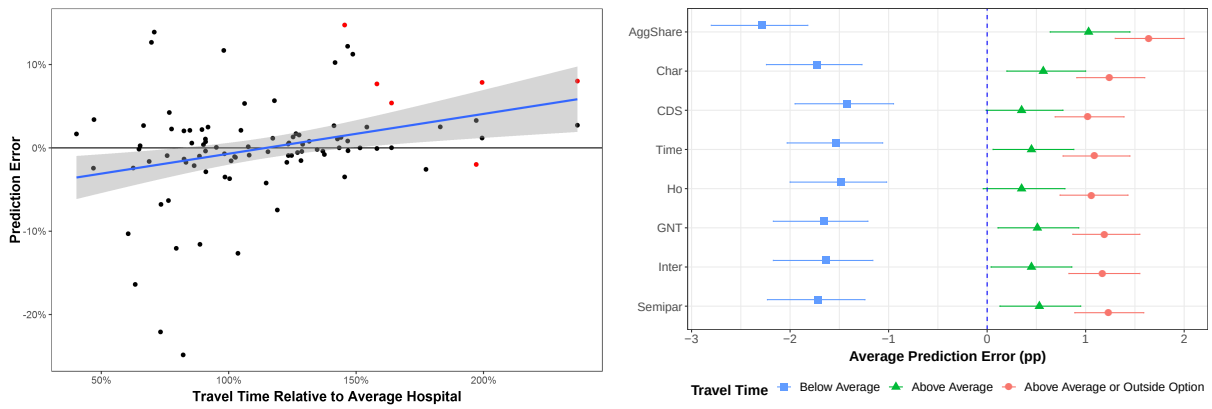

(a) By Model

(b) Average Prediction Error by Distance Group

Figure A-3 Prediction as a Function of Distance, Full Sample

Note: First panel shows the prediction error as a function of the average travel time to the hospital expressed as a percent of the average travel time in the market. Second panel presents the average prediction error, differentiating between hospitals whose travel time is below average for their market, above average for their market, or above average plus the Outside Option. Bars represent 95% confidence intervals computed from 200 bootstrap replications; we also apply a bootstrap bias correction. See Table A-13 for tables of the estimates and confidence intervals used to generate these figures.

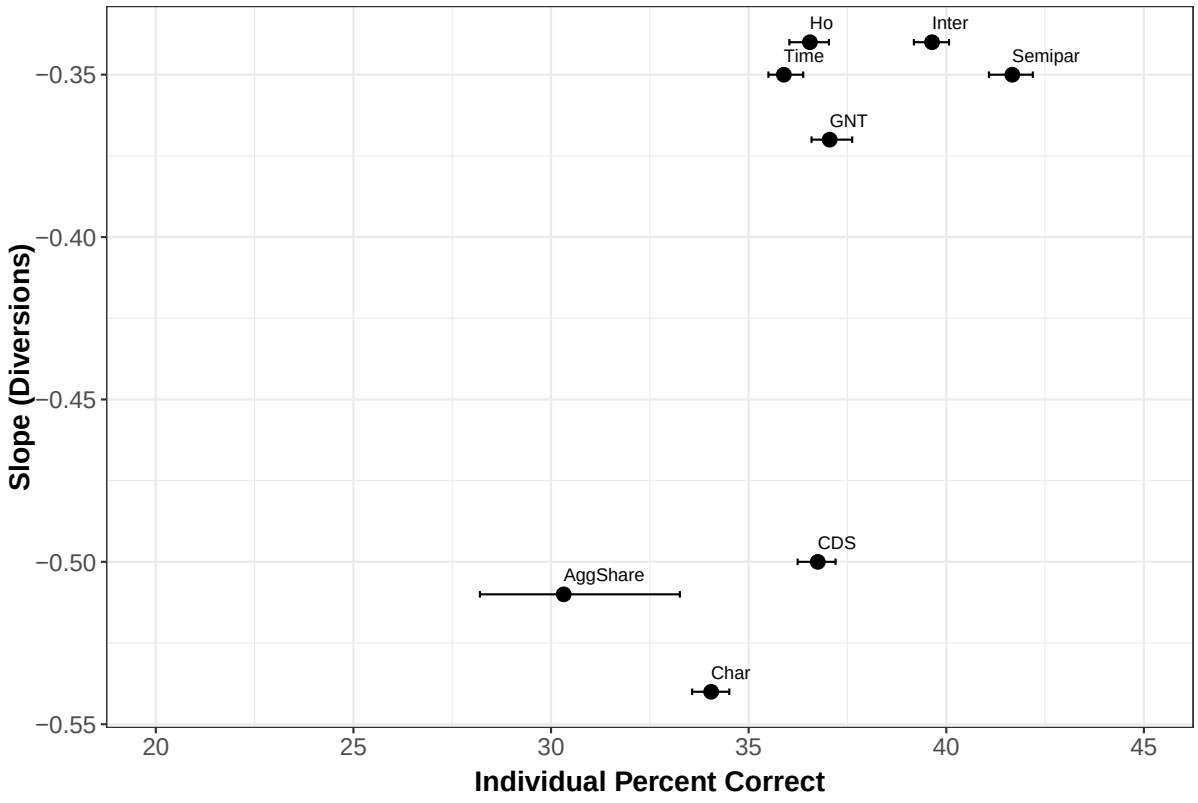

Figure A-4 Average Percent Correct of Individual Predictions vs. Slope Coefficient of Observed Diversion Ratio and Prediction Error, Full Sample

Note: The Figure compares the slope coefficient of the observed diversion ratio on the prediction error to the average percentage of individual choices correctly predicted. Bars represent 95% confidence intervals computed from 200 bootstrap replications; we also apply a bootstrap bias correction. See Table A-10 and Table A-14 for estimates and confidence intervals used to generate the figure.

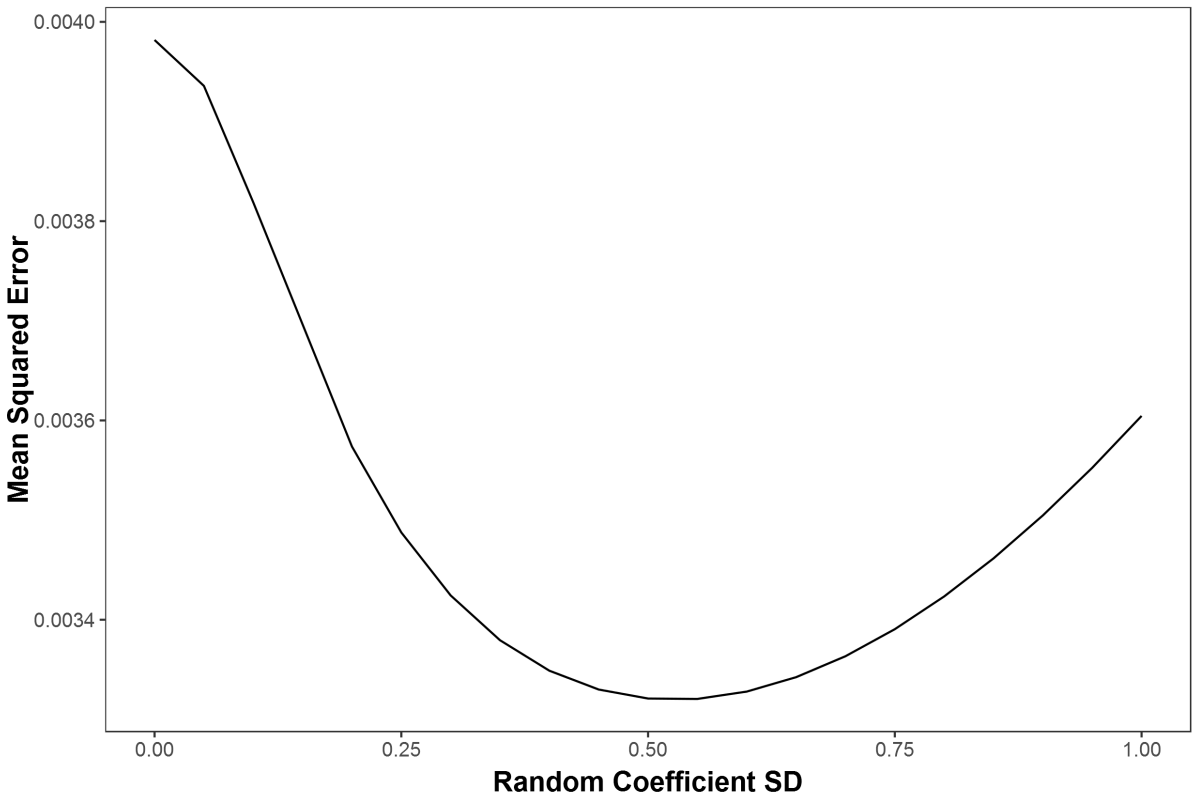

Figure A-5 MSE by Standard Deviation of Random Coefficient, Full Sample

Note: This figure shows the mean squared prediction error (MSE) of the *Common SD* class of models described in the text, where the models vary by the standard deviation of the random coefficient.

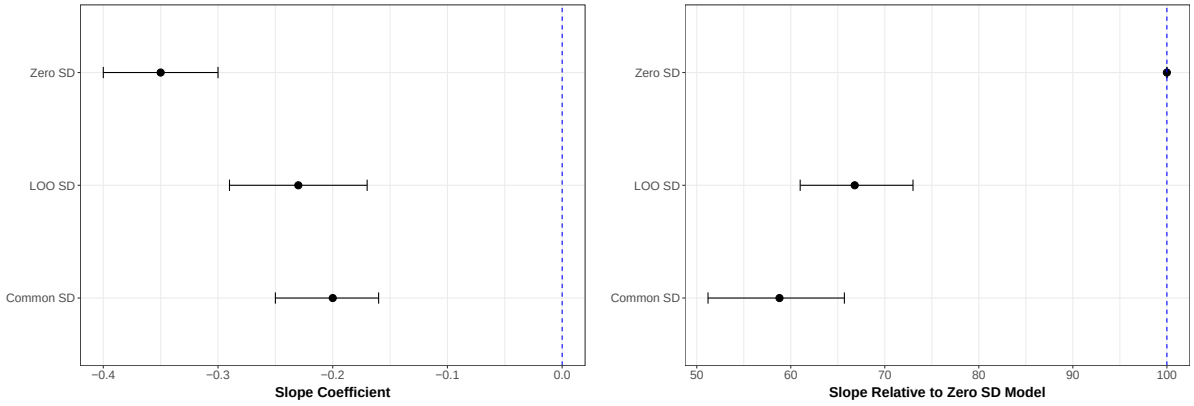

(a) By Model (b) Correlation by Distance

Figure A-6 Random Coefficient Relative Performance, Full Sample

Note: The left panel presents the slope of the observed diversion ratio on the prediction error. The right panel depicts the slope for a model relative to that for the Zero SD model. 95% confidence intervals are computed from 200 bootstrap replications; we also apply a bootstrap bias correction. See Table A-17 for estimates and confidence intervals used to generate the figure.

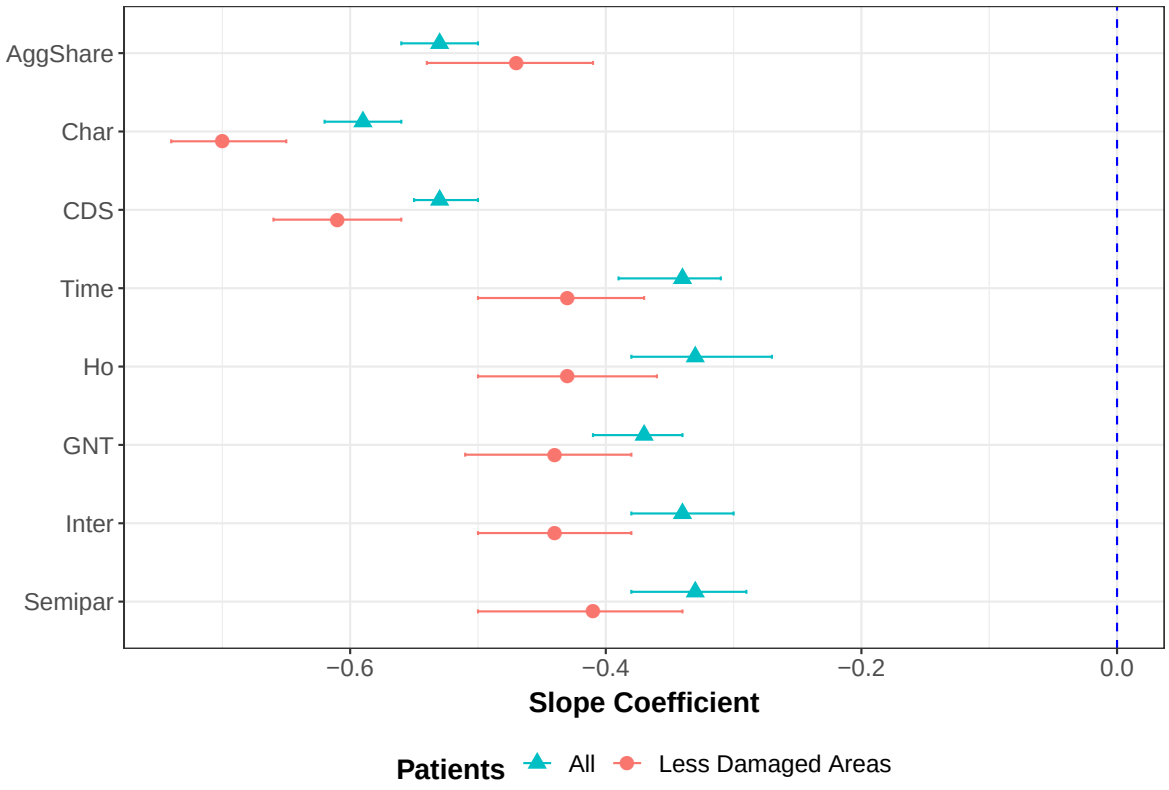

Figure A-7 Slope Coefficient of Observed Diversion Ratio on Prediction Error By Disaster Damage, Full Sample

Note: The figure depicts the slope of the observed diversion ratio on the prediction error. The figure only uses data from the Coney, St. John's, or Sumter experiments, and includes either all patients or patients in zip codes with less disaster damage. Bars represent 95% confidence intervals computed from 200 bootstrap replications; we also apply a bootstrap bias correction. See Table A-15, and Table A-16 for tables of the estimates and confidence intervals used to generate this figure.

G Supplemental Tables

G.1 Non-Elective Sample

Table A-1 Descriptive Statistics fo Affected Hospital Service Areas, Non-Elective Sample

	Pre-Period Admissions	Post-Period Admissions	Zip Codes	Choice Set Size	Outside Option Share	Destroyed Share	Destroyed Acuity
Sumter	5,197	3,951	11	15	3.1	51.2	0.97
StJohns	68,205	12,946	29	21	9.0	16.8	1.20
NYU	57,018	12,714	38	19	12.3	3.6	0.96
Moore	6,291	2,451	5	12	1.8	12.5	0.91
Coney	32,976	7,120	8	17	7.0	16.2	1.12
Bellevue	32,855	6,715	19	20	7.3	10.5	1.18

Note: The first column indicates the number of admissions in the pre-period data, the second column the number of admissions in the post-period data, the third column the number of zip codes in the service area, the fourth column the number of choices (including the outside option), the fifth column the share of admissions in the pre-period from the 90% service area that went to the outside option, the sixth column the share of admissions in the pre-period from the 90% service area that went to the destroyed hospital, and the seventh column the average DRG weight of admissions to the destroyed hospital in the pre-period data.

Table A-2 Slope Coefficient of Observed Choice Removal Diversion Ratios on Prediction Error, By Model, Non-Elective Sample

Model	Slope	Slope Rel to AggShare
AggShare	-0.58	100
	(-0.62,-0.54)	(100,100)
CDS	-0.58	99.3
	(-0.62,-0.54)	(96.8,101.6)
Char	-0.61	104.8
	(-0.65,-0.57)	(101.9,107.8)
Time	-0.43	75.1
	(-0.49,-0.38)	(70.8,79.8)
Ho	-0.42	72.2
	(-0.48,-0.36)	(67,77.3)
GNT	-0.44	76.6
	(-0.5,-0.39)	(72.8,80.2)
Inter	-0.42	72.2
	(-0.48,-0.36)	(67.4,77.2)
Semipar	-0.43	73.8
	(-0.49,-0.38)	(69.6,79.3)

Note: All results use data from all of the experiments. The second column presents the slope of the observed diversion ratio on the prediction error. The third column depicts the slope for a model relative to that for the *AggShare* model. The lower and upper bounds of the 95% confidence intervals, which are computed from 200 bootstrap replications, are shown below the average slope coefficients; we also apply a bootstrap bias correction.

Table A-3 Slope Coefficient of Observed Choice Removal Diversion Ratios on Prediction Error for *Semipar*, by Experiment, Non-Elective Sample

Experiment	Slope
Sumter	-0.11
	(-0.19,-0.03)
StJohns	-0.56
	(-0.65,-0.47)
NYU	-0.6
	(-0.72,-0.51)
Moore	-0.67
	(-0.78,-0.59)
Coney	-0.6
	(-0.65,-0.55)
Bellevue	0.07
	(-0.05,0.19)

Note: All results use data from all of the experiments for the *Semipar* model. The second column presents the slope of the observed diversion ratio on the prediction error. The lower and upper bounds of the 95% confidence intervals, which are computed from 200 bootstrap replications, are shown below the average slope coefficients; we also apply a bootstrap bias correction.

Table A-4 Decomposition of Average Predicted Diversion, Non-Elective Sample

Model	Individual	Individual + Heterogeneity Factor
AggShare	-0.58	-0.58
	(-0.62,-0.54)	(-0.62,-0.54)
CDS	-0.67	-0.58
	(-0.7,-0.64)	(-0.62,-0.54)
Char	-0.69	-0.61
	(-0.73,-0.66)	(-0.65,-0.57)
Time	-0.52	-0.43
	(-0.57,-0.47)	(-0.49,-0.38)
Ho	-0.51	-0.42
	(-0.57,-0.47)	(-0.48,-0.36)
GNT	-0.53	-0.44
	(-0.58,-0.48)	(-0.5,-0.39)
Inter	-0.51	-0.42
	(-0.56,-0.47)	(-0.48,-0.36)
Semipar	-0.51	-0.43
	(-0.56,-0.47)	(-0.49,-0.38)

Note: The second column depicts the slope of the observed diversion ratio on the prediction error based on the predicted individual diversion ratio, while the third column depicts the slope of the observed diversion ratio on the prediction error based on the predicted individual diversion ratio plus the heterogeneity factor. Each term is as defined in the text. 95% confidence intervals are computed from 200 bootstrap replications; we also apply a bootstrap bias correction.

Table A-5 Average Prediction Error by Average Hospital Distance, Non-Elective Sample

Model	Below Avg	Above Avg	Above Avg or Outside Option
AggShare	-1.79	0.49	1.28
	(-2.4,-1.25)	(0.04,0.92)	(0.9,1.71)
CDS	-1.04	-0.1	0.75
	(-1.64,-0.48)	(-0.57,0.35)	(0.35,1.17)
Char	-1.34	0.13	0.96
	(-1.94,-0.8)	(-0.34,0.56)	(0.58,1.38)
Time	-1.05	-0.07	0.75
	(-1.66,-0.51)	(-0.52,0.36)	(0.37,1.19)
Ho	-1.01	-0.16	0.73
	(-1.64,-0.43)	(-0.66,0.28)	(0.32,1.17)
GNT	-1.16	-0.02	0.83
	(-1.75,-0.61)	(-0.47,0.42)	(0.44,1.25)
Inter	-1.2	-0.04	0.86
	(-1.8,-0.65)	(-0.52,0.42)	(0.47,1.29)
Semipar	-1.2	0.04	0.86
	(-1.82,-0.63)	(-0.43,0.49)	(0.46,1.3)

Note: We report estimates of average prediction error, examining separately hospitals whose travel time is below average for their market, above average for their market, or above average plus the Outside Option. 95% confidence intervals are computed from 200 bootstrap replications; we also apply a bootstrap bias correction.

Table A-6 Predictive Accuracy – Averaged over all Experiments, Non-Elective Sample

Model	Percent Correct	RMSE
AggShare	25.28	0.2298
	(24.96,25.59)	(0.2295,0.23)
CDS	37.88	0.2179
	(37.55,38.25)	(0.2175,0.2184)
Char	34.14	0.2223
	(33.73,34.54)	(0.2219,0.2227)
Time	35.79	0.219
	(35.44,36.11)	(0.2186,0.2193)
Ho	38.5	0.2159
	(37.2,43.17)	(0.2112,0.2172)
GNT	37.55	0.218
	(37.21,37.94)	(0.2177,0.2184)
Inter	40.08	0.2142
	(39.7,41.09)	(0.2124,0.2147)
Semipar	41.62	0.2126
	(41.18,42.09)	(0.2121,0.2132)

Note: The second column is the average percent of individual predictions predicted correctly for each model; we define a prediction as correctly predicting if the patient goes to the hospital with the highest predicted probability, and average across experiments. The third column is the average RMSE for individual predictions, averaged across the different experiments. 95% confidence intervals are computed from 200 bootstrap replications; we also apply a bootstrap bias correction.

Table A-7 Slope Coefficient of Observed Choice Removal Diversion Ratios on Prediction Error, by Model, For Areas With Less Disaster Damage, Non-Elective Sample

Model	Slope	Slope Rel to AggShare
AggShare	-0.51	100
	(-0.58,-0.45)	(100,100)
CDS	-0.63	123
	(-0.68,-0.58)	(115.2,128.9)
Char	-0.72	140.2
	(-0.77,-0.67)	(129.1,149.1)
Time	-0.47	91.1
	(-0.54,-0.4)	(88.3,94.4)
Ho	-0.46	90.1
	(-0.54,-0.39)	(85.1,95.3)
GNT	-0.47	92.7
	(-0.55,-0.41)	(90.1,95.6)
Inter	-0.48	93.3
	(-0.55,-0.41)	(88.2,99.1)
Semipar	-0.46	89.7
	(-0.53,-0.38)	(81.7,97.2)

Note: Results based upon the Coney, St John's, and Sumter experiments for areas with less disaster damage, as defined in the text. The second column presents the slope of the observed diversion ratio on the prediction error. The third column depicts the slope for a model relative to that for the *AggShare* model; this value is thus 100 for *AggShare*. 95% confidence intervals are computed from 200 bootstrap replications; we also apply a bootstrap bias correction.

Table A-8 Slope Coefficient of Observed Choice Removal Diversion Ratios on Prediction Error, by Model, For Coney, St John's, and Sumter Experiments, Non-Elective Sample

Model	Slope	Slope Rel to AggShare
AggShare	-0.55	100
	(-0.58,-0.51)	(100,100)
CDS	-0.55	100
	(-0.58,-0.51)	(96.1,103.9)
Char	-0.6	109.9
	(-0.64,-0.56)	(104.4,114.5)
Time	-0.36	66.6
	(-0.4,-0.32)	(61.5,71.6)
Ho	-0.34	62.8
	(-0.39,-0.29)	(56,68.5)
GNT	-0.39	71.1
	(-0.43,-0.34)	(66.5,76.2)
Inter	-0.36	66.5
	(-0.41,-0.31)	(58.7,72.2)
Semipar	-0.37	67.5
	(-0.41,-0.31)	(59.9,74.6)

Note: Results based upon the Coney, St John's, and Sumter experiments using all zip codes in the relevant service area. The second column presents the slope of the observed diversion ratio on the prediction error. The third column depicts the slope for a model relative to that for the *AggShare* model. 95% confidence intervals are computed from 200 bootstrap replications; we also apply a bootstrap bias correction.

Table A-9 Slope Coefficient of Observed Choice Removal Diversion Ratios on Prediction Error, by Random Coefficient Model, Non-Elective Sample

Model	Slope	Slope Rel to Zero SD
Zero SD	-0.43	100
	(-0.49,-0.38)	(100,100)
LOO Common SD	-0.35	80.2
	(-0.41,-0.28)	(75.6,85.4)
Common SD	-0.32	74
	(-0.37,-0.27)	(67.4,79.6)

Note: The second column presents the slope of the observed diversion ratio on the prediction error. The third column depicts the slope for a model relative to that for the Zero SD model. 95% confidence intervals are computed from 200 bootstrap replications; we also apply a bootstrap bias correction.

G.2 Full Sample

Table A-10 Slope Coefficient of Observed Choice Removal Diversion Ratios on Prediction Error, By Model, By Model, Full Sample

Model	Slope	Slope Rel to AggShare
AggShare	-0.51	100
	(-0.55,-0.47)	(100,100)
CDS	-0.5	97.5
	(-0.53,-0.46)	(95.3,99.6)
Char	-0.54	105.8
	(-0.58,-0.51)	(102.9,108.4)
Time	-0.35	68.2
	(-0.4,-0.3)	(63.9,72.9)
Ho	-0.34	65.7
	(-0.39,-0.28)	(60.3,70.7)
GNT	-0.37	73
	(-0.42,-0.33)	(68.9,76.9)
Inter	-0.34	67.2
	(-0.39,-0.3)	(62.9,71.9)
Semipar	-0.35	67.9
	(-0.39,-0.3)	(63,73.3)

Note: All results use data from all of the experiments. The second column presents the slope of the observed diversion ratio on the prediction error. The third column depicts the slope for a model relative to that for the *AggShare* model. The lower and upper bounds of the 95% confidence intervals, which are computed from 200 bootstrap replications, are shown below the average slope coefficients; we also apply a bootstrap bias correction.

Table A-11 Slope Coefficient of Observed Choice Removal Diversion Ratios on Prediction Error for *Semipar*, by Experiment, Full Sample

Experiment	Correlation
Sumter	-0.21
	(-0.27,-0.14)
StJohns	-0.44
	(-0.52,-0.37)
NYU	-0.26
	(-0.36,-0.16)
Moore	-0.63
	(-0.74,-0.54)
Coney	-0.5
	(-0.56,-0.44)
Bellevue	0
	(-0.1,0.11)

Note: All results use data from all of the experiments for the *Semipar* model. The second column presents the slope of the observed diversion ratio on the prediction error. The lower and upper bounds of the 95% confidence intervals, which are computed from 200 bootstrap replications, are shown below the average slope coefficients; we also apply a bootstrap bias correction.

Table A-12 Decomposition of Average Predicted Diversion, Full Sample

Model	Individual	Individual + Heterogeneity Factor
AggShare	-0.51	-0.51
	(-0.55,-0.47)	(-0.55,-0.47)
CDS	-0.61	-0.5
	(-0.64,-0.58)	(-0.53,-0.46)
Char	-0.64	-0.54
	(-0.67,-0.61)	(-0.58,-0.51)
Time	-0.45	-0.35
	(-0.49,-0.41)	(-0.4,-0.3)
Ho	-0.45	-0.34
	(-0.49,-0.4)	(-0.39,-0.28)
GNT	-0.46	-0.37
	(-0.5,-0.42)	(-0.42,-0.33)
Inter	-0.44	-0.34
	(-0.49,-0.4)	(-0.39,-0.3)
Semipar	-0.44	-0.35
	(-0.48,-0.4)	(-0.39,-0.3)

Note: The second column depicts the slope of the observed diversion ratio on the prediction error based on the predicted individual diversion ratio, while the third column depicts the slope of the observed diversion ratio on the prediction error based on the predicted individual diversion ratio plus the heterogeneity factor. Each term is as defined in the text. 95% confidence intervals are computed from 200 bootstrap replications; we also apply a bootstrap bias correction.

Table A-13 Average Prediction Error by Average Hospital Distance, Full Sample

Model	Below Avg	Above Avg	Above Avg or Outside Option
AggShare	-2.29	1.03	1.64
	(-2.8,-1.82)	(0.64,1.45)	(1.3,2)
CDS	-1.42	0.35	1.02
	(-1.95,-0.95)	(-0.01,0.77)	(0.69,1.39)
Char	-1.73	0.57	1.24
	(-2.24,-1.27)	(0.2,1)	(0.91,1.6)
Time	-1.53	0.45	1.09
	(-2.03,-1.06)	(0.06,0.88)	(0.77,1.45)
Ho	-1.48	0.35	1.06
	(-2,-1.02)	(-0.04,0.79)	(0.74,1.43)
GNT	-1.66	0.51	1.19
	(-2.17,-1.21)	(0.11,0.93)	(0.87,1.55)
Inter	-1.64	0.45	1.17
	(-2.17,-1.16)	(0.04,0.86)	(0.83,1.55)
Semipar	-1.72	0.53	1.23
	(-2.23,-1.24)	(0.13,0.95)	(0.89,1.59)

Note: We report estimates of average prediction error, examining separately hospitals whose travel time is below average for their market, above average for their market, or above average plus the Outside Option. 95% confidence intervals are computed from 200 bootstrap replications; we also apply a bootstrap bias correction.

Table A-14 Predictive Accuracy – Averaged over all Experiments, Full Sample

Model	Percent Correct	RMSE
AggShare	30.25	0.236
	(28.16,33.25)	(0.2358,0.2363)
CDS	36.73	0.2259
	(36.18,37.24)	(0.2254,0.2264)
Char	34.06	0.2302
	(33.54,34.58)	(0.2298,0.2307)
Time	35.86	0.2256
	(35.38,36.33)	(0.2251,0.226)
Ho	36.54	0.2242
	(36.02,37.08)	(0.2236,0.2247)
GNT	37	0.2254
	(36.56,37.5)	(0.2249,0.226)
Inter	39.6	0.2211
	(39.14,40.04)	(0.2206,0.2216)
Semipar	42.26	0.2188
	(41.76,42.83)	(0.2179,0.2196)

Note: The second column is the average percent of individual predictions predicted correctly for each model; we define a prediction as correctly predicting if the patient goes to the hospital with the highest predicted probability, and average across experiments. The third column is the average RMSE for individual predictions, averaged across the different experiments. 95% confidence intervals are computed from 200 bootstrap replications; we also apply a bootstrap bias correction.

Table A-15 Slope Coefficient of Observed Choice Removal Diversion Ratios on Prediction Error, by Model, For Areas With Less Disaster Damage, Full Sample

Model	Slope	Slope Rel to AggShare
AggShare	-0.47	100
	(-0.54,-0.41)	(100,100)
CDS	-0.61	129.5
	(-0.66,-0.56)	(120.9,134.9)
Char	-0.7	148
	(-0.74,-0.65)	(136.1,157.6)
Time	-0.43	92
	(-0.5,-0.37)	(90.1,94.5)
Ho	-0.43	90.9
	(-0.5,-0.36)	(85.5,94.9)
GNT	-0.44	94.3
	(-0.51,-0.38)	(92.2,96.8)
Inter	-0.44	93.3
	(-0.5,-0.38)	(89.3,98.1)
Semipar	-0.41	87.5
	(-0.5,-0.34)	(79.3,95.7)

Note: Results based upon the Coney, St John's, and Sumter experiments for areas with less disaster damage, as defined in the text. The second column presents the slope of the observed diversion ratio on the prediction error. The third column depicts the slope for a model relative to that for the *AggShare* model; this value is thus 100 for *AggShare*. 95% confidence intervals are computed from 200 bootstrap replications; we also apply a bootstrap bias correction.

Table A-16 Slope Coefficient of Observed Choice Removal Diversion Ratios on Prediction Error, by Model, For Coney, St John's, and Sumter Experiments, Full Sample

Model	Slope	Slope Rel to AggShare
AggShare	-0.53	100
	(-0.56,-0.5)	(100,100)
CDS	-0.53	99.9
	(-0.55,-0.5)	(97,102.9)
Char	-0.59	111.6
	(-0.62,-0.56)	(107.8,115.5)
Time	-0.34	64.9
	(-0.39,-0.31)	(60.8,70)
Ho	-0.33	62
	(-0.38,-0.27)	(53.4,67.8)
GNT	-0.37	70.6
	(-0.41,-0.34)	(66.4,75.1)
Inter	-0.34	63.9
	(-0.38,-0.3)	(58.8,69)
Semipar	-0.33	62.9
	(-0.38,-0.29)	(57,69.4)

Note: Results based upon the Coney, St John's, and Sumter experiments using all zip codes in the relevant service area. The second column presents the slope of the observed diversion ratio on the prediction error. The third column depicts the slope for a model relative to that for the *AggShare* model. 95% confidence intervals are computed from 200 bootstrap replications; we also apply a bootstrap bias correction.

Table A-17 Slope Coefficient of Observed Choice Removal Diversion Ratios on Prediction Error, by Random Coefficient Model, Full Sample

Model	Slope	Slope Rel to Zero SD
Zero SD	-0.35	100
	(-0.4,-0.3)	(100,100)
LOO Common SD	-0.23	66.8
	(-0.29,-0.17)	(61,73)
Common SD	-0.2	58.8
	(-0.25,-0.16)	(51.2,65.7)

Note: The second column presents the slope of the observed diversion ratio on the prediction error. The third column depicts the slope for a model relative to that for the Zero SD model. 95% confidence intervals are computed from 200 bootstrap replications; we also apply a bootstrap bias correction.

H Table of Variables Used

	AggShare	Char	CDS	Time	Ho	GNT	Inter
Hospital Indicators	X			X	X	X	X
× Weight						X	X
× Time							X
× Obstetrics							X
× Circulatory							X
× Digest							X
× Muscular							X
× Respiratory							X
× Female Repro							X
Inside		X	X				
× Cardiac Surg Diag			X				
Same County			X				
Time		X	X	X	X	X	X
× Median Income			X			X	
× LOS			X				
× nPX			X				
× nDX			X				
× Emergency			X		X		
× Medical			X				
× Obstetrics			X				X
× Weight		X	X			X	X
× Age						X	

	AggShare	Char	CDS	Time	Ho	GNT	Inter
× Under18			X				X
× Over64		X	X			X	X
× Female		X	X			X	X
× Black							X
× Cardiac Surg Diag			X				
× Circulatory			X				X
× Digest			X				X
× Muscular			X				X
× Respiratory			X				X
× Female Repro			X				X
× RN Share			X				
× Teach			X				
× RN Intense			X				
× For Profit						X	
× Beds						X	
× Residents Per Bed						X	
× Teach						X	
Squared Time		X	X	X	X	X	X
× Weight		X					X
× Over64		X					X
× Under18							X
× Female		X					X
× Black							X

	AggShare	Char	CDS	Time	Ho	GNT	Inter
× Obstetrics							X
× Circulatory							X
× Digest							X
× Muscular							X
× Respiratory							X
× Female Repro							X
Closest						X	
Cardiac Surg Hosp							
× Cardiac Surg Diag × Adult		X					
× Weight × Adult		X					
Obstetrics Hosp							
× Obstetrics Diag		X					
× Female		X					
NICU Hosp							
× Female		X					
× Obstetrics Diag						X	
Residents/Bed							
× Weight		X					
× Over64		X					
× Female		X					
RN Share							
× Female			X				

	AggShare	Char	CDS	Time	Ho	GNT	Inter
× Over64			X				
× Median Income			X				
× LOS			X				
× nPX			X				
× nDX			X				
× Under18			X				
RN Int							
× Female			X				
× Over64			X				
× Median Income			X				
× LOS			X				
× nPX			X				
× nDX			X				
× Under18			X				
RN/Bed							
× Commercial					X		
× Cardiac					X		
× Oncology Alt					X		
× Neurology					X		
× Digest Alt					X		
× Labor and Delivery					X		
× Median Income					X		
For Profit							

	AggShare	Char	CDS	Time	Ho	GNT	Inter
× Weight		X					
× Over64		X					
× Female		X					
× Commercial					X		
× Cardiac					X		
× Oncology Alt					X		
× Neurology					X		
× Digest Alt					X		
× Labor and Delivery					X		
× Median Income					X		
Imaging Complexity							
× Commercial					X		
× Cardiac					X		
× Oncology Alt					X		
× Neurology					X		
× Digest Alt					X		
× Labor and Delivery					X		
× Median Income					X		
Teach							
× Female			X				
× Old			X				
× LOS			X				
× nPX			X				

	AggShare	Char	CDS	Time	Ho	GNT	Inter
× nDX			X				
× Under18			X				
× Commercial					X		
× Cardiac					X		
× Oncology Alt					X		
× Neurology					X		
× Digest Alt					X		
× Labor and Delivery					X		
× Median Income			X		X		
Cardiac Complexity							
× Commercial					X		
× Cardiac					X		
× Median Income					X		
× Commercial					X		
× Oncology Alt					X		
× Median Income					X		
Birth Complexity							
× Commercial					X		
× Labor and Delivery					X		
× Median Income					X		
Oncology Diag × Cancer Center			X				
Delivery × Birth Room			X				
Circulatory × Cardiac ICU			X				

	AggShare	Char	CDS	Time	Ho	GNT	Inter
Circulatory × Cath Lab						X	
Under18 × Ped Beds			X				
Trauma × CTC			X				
Imaging Diag × MRI						X	

Variable	Source	Description
Adult	Disch	Age greater than 17
Age	Disch	Patient age
Beds	AHA	Number of beds in hospital
Black	Disch	Patient is racially black
Birth Room	AHA	Whether hospital has birthing (LDR, LDRP) room
Birth Complexity	AHA	We apply the Ho services intensity algorithm (see below) to the obstetrics and birth room flags from the AHA data
Cardiac Surg Diag	Disch	For V24 DRG coding: DRGs between 215 and 236; Between V24 and V12: DRGs in this list (104,105,106,108,515,525,535,536,547,548,549,550); Below V12: DRGs between 103 and 107, 207[44]
Cardiac Surg Hosp	AHA	Whether hospital has an cardiac surgery program
Cardiac Diagnosis	Disch	3 digit ICD9 diagnosis codes between (and including) 393 and 398, 401 and 405, 410-417, 420-429
Cardiac ICU	AHA	Whether hospital has cardiac ICU
Cardiac Complexity	AHA	We apply the Ho services intensity algorithm (see below) to adult diagnostic catheterization, cardiac intensive care, adult interventional cardiac catheterization, and adult cardiac surgery flags from the AHA data
Cath Lab	AHA	Whether a hospital has both a diagnostic and interventional catheterization lab
Cancer Center	AHA	Whether hospital has oncology services
Cancer Complexity	AHA	We apply the Ho services intensity algorithm (see below) to the cancer and maximum of the image-guided radiation and intensity-modulated radiation flags from the AHA data

[44]Across the models, three different underlying variables are based on the patient's diagnosis. First, the discharge data include ICD9 diagnosis codes for patients; these diagnosis codes, along with other variables such as procedures, age, sex, discharge status, and the presence of complications or comorbidities, are used to assign a Diagnosis Research Group or DRG. The DRGs themselves are grouped into 25 different Major Diagnosis Categories or MDCs. For example, a patient presenting signs of "maple syrup urine disease" would have ICD9 diagnosis code 270.3, DRG 642 (Inborn and other disorders of metabolism), and MDC 10 (Diseases and Disorders of the Endocrine, Nutritional And Metabolic System).

Closest	Disch	Whether hospital is closest facility to patient
Circulatory	Disch	MDC equals 5
Commercial	Disch	Patient has a commercial insurer
CTC	AHA	Certified Trauma Center
Delivery	Disch	For DRG coding above V24: DRGs in this list (765, 766, 774, 775, 767, 768, 776, 769, 777, 780, 781, or 782). For DRG coding below V12: DRGs from 370-378 and 382-384
Digest	Disch	MDC equals 6
Digest Alt	Disch	3 digit ICD9 diagnosis codes between (inclusive) 520 and 579
Emergency	Disch	Patient admitted through emergency room
Female	Disch	Patient is female
Female Repro	Disch	MDC equals 13
For Profit	AHA	Whether hospital is a for profit facility
Imaging Complexity	AHA	We apply the Ho services intensity algorithm (see below) to SPECT, MRI, CT, ultrasound, and PET scan flags from the AHA survey
Imaging Diag	Disch	MDC code is 1, 5, or 8
Labor and Delivery	Disch	ICD9 diagnosis codes between (inclusive) 650 and 657, 644, 647, 648, V22, V23, V24, V27
Inside	NA	Hospital is not the outside option
Median Income	ACS	Median income of zip code
Medical	Disch	Medical DRG
MRI	AHA	Hospital has an MRI
Muscular	Disch	MDC equals 8
nDX	Disch	Number of diagnoses
nPX	Disch	Number of procedures
LOS	Disch	Length of stay
Neurology	Disch	3 digit ICD9 diagnosis codes between 320 and 326, 330 and 337, or 340 and 359 (inclusive)
NICU Diag	Disch	For V24 DRG Coding: DRG 790 or 791; Pre V24: DRG 386 or 387
NICU Hosp	AHA	Hospital has a NICU
Obstetrics Diag	Disch	MDC equals 14
Obstetrics Hosp	AHA	Hospital has an obstetrics program
Oncology Diag	Disch	MDC equals 17 or for DRG later than V24 in this list (54, 55, 146, 147, 148, 180, 181, 182, 374, 375, 376, 420, 421, 422, 435, 436, 437, 542, 543, 544, 582, 583, 584, 585, 597, 598, 599, 656, 657, 658, 686, 687, 688, 711, 712, 715, 716, 722, 723, 724, 739, 740, 741, 736, 737, 738, 744, 745, 754, 755, 756, 843, 844, 835, 836, 837, 838, or 839). For DRG pre V12 in this list (10, 11, 64, 82, 172, 173, 199, 203, 239, 257, 258, 259, 260, 274, 275, 303, 318, 319, 338, 344, 346, 347, 354, 355, 357, 363, 366, 367, 406, 407, 408, 413, 414).
Oncology Alt	Disch	3 digit ICD9 diagnosis codes between 140 and 239 (inclusive)

Over64	Disch	Patient is over 64 years old
PatCounty	Disch	Patient's County of Residence
Ped Beds	Disch	Hospital has pediatric beds
Respiratory	Disch	MDC equals 4
Residents Per Bed	MCR	Residents per bed from Medicare Cost Reports
RN Share	AHA	Nurses regularly working as a share of licensed nurses
RN Intense	AHA	Nurses regularly working as share of inpatient days
RN/Bed	AHA	Nurses per bed
Same County	Disch	Hospital and patient in same county
Teach	AHA	Teaching hospital
Trauma	Disch	MDC equals 24
Time	Disch/Compute	Travel time from centroid of patients zip code to hospital
Under18	Disch	Patient is under 18
Weight	Disch	DRG weight

Description of Ho Services Intensity Algorithm: Hospitals were rated on a scale of zero to one, reflecting the sophistication of their services in different categories. Zero indicates low sophistication and one indicates a high level of sophistication. The four categories are cardiac, imaging, cancer, births.

The intensity variable for category c in hospital h is given by:

$$\max\{\max_{x \in X_c} 1_{xh} * (1 - \bar{x})(1 - \bar{y_c}), 1_{yh_c}\}$$

where

- x indexes the services in each category
- 1_{xh} is 1 if hospital h offers service x and 0 if not
- $\bar{x}$ is the state share of hospitals offering that service
- y is the service with the smallest $\bar{x}$
- 1_{yh} is 1 if hospital h offers service y and 0 if not
- $\bar{y}$ is the percent of hospitals offering service y

For more details see Table IX in Ho (2006).